Supporting information for:

Lanthanide appended rotaxanes respond to changing chloride concentration

Clémence Allain,[a] Paul D. Beer,[a]* Stephen Faulkner,[a]* Michael W. Jones,[a] Alan M. Kenwright,[b] Nathan L. Kilah,[a] Richard C. Knighton,[a] Thomas Just Sørensen[a] and Manuel Tropiano [a]

Table of Contents

Synthetic procedures

Commercially available solvents and chemicals were used without further purification unless otherwise stated. Where dry solvents were used, they were degassed with nitrogen, dried by passing through an MBraun MPSP-800 column and then used immediately. Triethylamine was distilled from and stored over potassium hydroxide. Water was deionised and microfiltered using a Milli-Q Millipore machine. Tetrabutylammonium (TBA) salts were stored under vacuum in a desiccator. Routine 300 MHz NMR spectra were recorded on a Varian Mercury 300 spectrometer, ^{1}H NMR operating at 300 MHz, ^{13}C at 75.5 MHz. All 500 MHz ^{1}H Spectra and all ^{1}H NMR titrations were recorded on a Varian Unity Plus 500 spectrometer. 700 MHz ^{1}H Spectra were recorded on a Varian VNMRS-700. All chemical shift (δ) values are given in parts per million.

Low resolution mass spectra were recorded on a Micromass LCT Premier XE spectrometer. Accurate masses were determined to four decimal places using Bruker μTOF and Micromass GCT spectrometers. Luminescence spectra were measured on a Horiba Jobin Yvon FluoroLog-3 equipped with a Hamamatsu R928 PMT detector and a double-grating emission monochromator. In the case of the ytterbium complex, the sample was excited using a pulsed nitrogen laser (PTI-3301-337nm. Light emitted at right angles to the excitation beam was focused onto the slits of the monochromator (PTI120), which was used to select the appropriate wavelength. The growth and decay of the luminescence at selected wavelengths was detected using a germanium photodiode (Edinburgh Instruments, EI-P) and recorded using a digital oscilloscope (Tektronix TDS220) before being transferred to the computer for analysis. Luminescence lifetimes were obtained by iterative reconvolution of the detector response (obtained by using a scatter) with exponential components for growth and decay of the metal centred luminescence for ytterbium complexes or by tail fit for europium complexes, using a spreadsheet running in Microsoft Excel.

Synthesis

Compounds **2**[1], **3**[2], Eu·**5** and Lu·**5**[3] were synthesised according to literature procedures.

WARNING: organic azides are potentially explosive substances and proper safety precautions should be taken when handling these compounds.

Synthesis of 5-azidoisophthalic acid

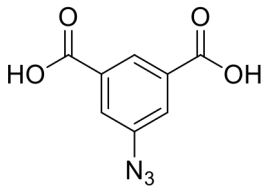

A solution of sodium nitrite (3.81 g, 55.2 mmol) dissolved in water (50 mL) at 0 °C was added over two minutes to a suspension of 5-aminoisophthalic acid (10.0 g, 55.2 mmol) in 1:1 conc. hydrochloric acid/water mixture (80 mL) at 0 °C. After stirring for an additional 3 min, a solution of sodium azide (3.59 g, mmol) and sodium acetate trihydrate (53.3 g, 392 mmol) in water (15 mL) at 0 °C was added carefully. The reaction mixture was stirred for 30 min and extracted with ethyl acetate (3 x 200 mL). The organic phases were combined, dried ($MgSO_4$), filtered and the solvent removed *in vacuo*. The isolated solid was triturated with diethyl ether, collected and dried *in vacuo* to give an off white solid(9.03 g (79%). ^{1}H NMR (300MHz, DMSO-d_6) 13.05 (2H, s), 7.97 (1H, s), 7.50 (2H, s). ^{13}C NMR (300MHz, DMSO- d_6) 165.7, 140.6, 132.9, 126.1, 123.4. LRMS (ESI): *m/z*: calcd for $C_8H_5N_3O_4$: 207; found: 207 [M-H]+.

Synthesis of azide rotaxane 4.Cl

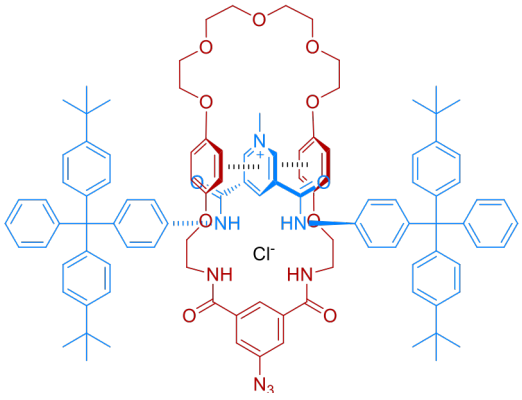

Axle **2**·Cl (248 mg, 0.23 mmol) and bis-amine **3** (107 mg, 0.23 mmol) were dissolved in dry DCM (50 mL) and stirred for 5 minutes under a nitrogen atmosphere. Triethylamine (74 µL, 0.58 mmol) and 5-azidoisophthaloyl dichloride (58 mg, 0.023 mmol) in anhydrous DCM (20mL) were then added. The reaction was stirred at room temperature for 2 hours after which the solvent was removed *in vacuo*. The crude mixture was purified by column chromatography (silica; 97.5:2.5 $CHCl_3$/MeOH) followed by preparative TLC (silica; 97.5:2.5 $CHCl_3$/MeOH) to give **4**·Cl as a yellow solid (152 mg, 39%). ^{1}H NMR

(500MHz, $CDCl_3$) 10.38 (s, 2H, axle NH), 10.11 (s, 1H, pyridinium Ar*H*), 9.01 (s, 2H, pyridinium Ar*H*), 8.77 (s, 1H, isophthalamide Ar*H*), 8.54 (s, 2H, isophthalamide N*H*), 7.87 (d, ^3J = 9.0Hz, 4H, Ar*H*NH), 7.75 (2H, s, isophthalamide N*H*),7.27-7.04 (m, 34H, Ar*H*) 6.47 (d, ^3J = 8.5Hz, 4H, hydroquinone Ar*H*), 6.17 (d, ^3J = 8.5Hz, 4H, hydroquinone Ar*H*), 4.68 (s, 3H, N^+-C*H*$_3$), 4.11 (t, ^3J = 5.0Hz, 4H, -OC*H*$_2$-), 3.79-3.66 (m, 20H, -OC*H*$_2$-), 1.29 (s, 36H, ^{t}Bu). ^{13}C NMR (75MHz, $CDCl_3$) 166.1, 159.0, 153.3, 151.9, 149.0, 147.0, 146.5, 143.6, 141.9, 136.2, 134.7, 132.4, 131.3, 130.9, 127.7, 126.2, 124.6, 122.5, 120.0, 116.3, 115.0, 70.9, 70.7, 70.4, 67.7, 67.3, 64.1, 49.6, 40.0, 34.6, 31.6. HRMS (ESI): *m/z*: calcd. for $C_{106}H_{115}N_8O_4$: 1675.8680; found: 1675.8666 $[M\text{-}Cl]^+$.

Synthesis of azide rotaxane 4·PF_6

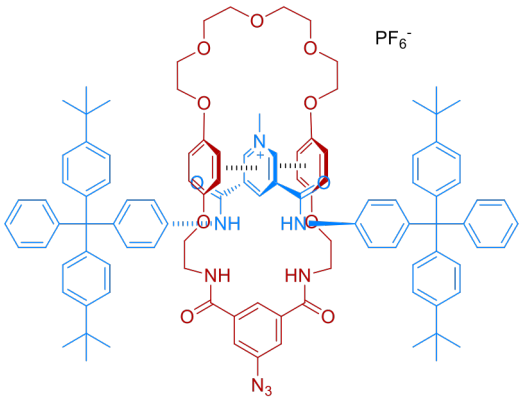

4·Cl rotaxane was dissolved in $CHCl_3$ (15 mL) and washed with NH_4PF_6(aq) solution (0.1M; 10 × 10 mL) and H_2O (2 × 10 mL). The organic layer was dried over $MgSO_4$ and the solvent removed *in vacuo* to give a yellow solid in quantitative yield. ^{1}H NMR (500MHz, $CDCl_3$) 9.28 (s, 1H, pyridinium Ar*H*), 8.73 (s, 2H, pyridinium Ar*H*), 7.96 (s, 1H, isophthalamide Ar*H*), 7.82 (s, 2H, isophthalamide Ar*H*), 7.65 (d, ^{3}J = 7.5, 4H, Ar*H*NH), 7.32-7.03 (m, 34H, Ar*H*), 6.62 (d, ^{3}J = 8.0Hz, 4H, hydroquinone Ar*H*), 6.35 (d, ^{3}J = 8.0Hz, 4H, hydroquinone Ar*H*), 4.16 (s, 3H, N^+-C*H*$_3$), 3.99 (s, 4H, -OC*H*$_2$-), 3.75-3.64 (m, 16H, -OC*H*$_2$-), 3.56 (s, 4H, -OC*H*$_2$-), 1.29 (s, 36H, ^{t}Bu). ^{13}C NMR (75MHz, $CDCl_3$) 166.1, 159.0, 153.3, 151.9, 149.0, 147.0, 145.5, 143.6, 141.9, 136.2, 134.7, 134.2, 132.4, 131.3, 130.9, 127.7, 126.2, 124.6, 122.5, 120.0, 119.5, 116.3, 115.0, 70.9, 70.7, 70.4, 67.7, 67.3, 64.1, 49.6, 40.0, 34.6, 31.6. HRMS (ESI): *m/z*: calcd. for $C_{106}H_{115}N_8O_4$: 1675.8680; found: 1675.8667 $[M\text{-}PF_6]^+$.

Synthesis of azidobenzene[4]

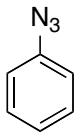

Aniline (204 mg, 2.2 mmol) was dissolved in anhydrous acetonitrile (6 mL) and this solution was left to cool in an ice-water bath for ten minutes. To this *t*-BuONO was added (340 mg, 3.3 mmol) followed by dropwise addition of $TMSN_3$ (305 mg, 2.6 mmol). After stirring under nitrogen atmosphere at room temperature for 1 h 30 minutes, the solvents were removed *in vacuo* and the product was purified by silica gel chromatography (hexane) to obtain a pale yellow oil (224 mg, 86%). ^{1}H-NMR (300 MHz; $CDCl_3$, ppm): 7.38-7.33 (m, 2H), 7.14 (td, J = 7.4, 1.3 Hz, 1H), 7.05-7.02 (m, 2H).

Synthesis of model compound 6

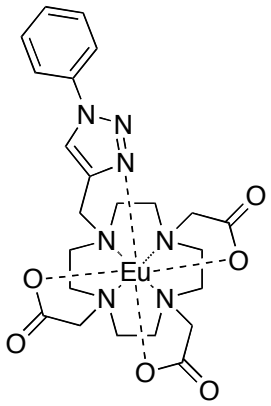

Eu·**5** (44 mg, 0.08 mmol) was dissolved in water (2.5 mL) and to this azidobenzene (20 mg, 0.17 mmol), dissolved in *tert*-butanol (2.5 mL), was added, followed by sodium ascorbate (2 mg, 0.008 mmol) and $CuSO_4$ (41 µL of a 0.1 M solution in water). This solution was left stirring at room temperature under nitrogen atmosphere for 48 h. The solvents were then removed and the solid obtained was washed with diethyl ether to remove excess of azidobenzene and the residual solids were redissolved in water and subjected to purification by dialysis for 3 days. HRMS [ES$^+$] calcd. for $C_{23}H_{30}EuN_7NaO_6$ 676.1364 *m/z* [M+Na]$^+$, found 676.1382 *m/z*. ^{1}H-NMR (300 MHz; D_2O, pD8, ppm): -19.39, -18.42, -11.16, -8.49, -4.96, 11.68, 25.86, 26.70, 27.13, 29.62. Lifetimes: H_2O: 0.54 ms; D_2O: 1.69 ms, q: 1.2.

General Procedure for the Synthesis of Lanthanide Rotaxane

To a solution of azide rotaxane **4**·PF_6 in CH_2Cl_2/MeOH (4:1, 5 mL) was added the appropriate lanthanide complex Ln·**5** (3 molar eq.). The solution was stirred for 5 minutes before $Cu^I(MeCN)_4PF_6$ (0.1 molar eq.) and tris[(1-benzyl-1*H*-1,2,3-triazol-4-yl)methyl]amine (0.1 molar eq.) were added. The solution was

stirred for 48 hours at room temperature in a nitrogen atmosphere after which the solvent was removed *in vacuo*. The crude solid was dissolved in DCM (10 mL) and the organic phase was washed with H_2O (2 × 10 mL), with an NH_4PF_6(aq) solution (0.1M; 10 × 10 mL) and H_2O (2 × 10 mL) to ensure the presence of only PF_6^- as the counter ion. After removal of the organic solvent *in vacuo* the crude solid was redissolved in toluene and filtered. Purification by size-exclusion chromatography (Bio-Beads SX-3/ toluene) gave the compound as a yellow solid.

Eu·1

HRMS [ES^+] calcd. for $C_{123}H_{140}EuN_{12}NaO_{17}$ 1116.9766 *m/z* $[M\text{-}PF_6+Na]^{2+}$, found 1116.9801 *m/z*. ^{1}H-NMR (500 MHz; 293 K CD_3OD/DCM 1:1, ppm): δ 34.25, 30.13, 29.97, 27.92, -3.99, -4.73, -5.54, -6.14, -7.46, -8.06, -8.65, -11.77, -12.33, -16.16, -16.44, -17.18, -17.74, -19.70, -21.14. Lifetimes: DCM: 0.85 ms.

Characterization

^{1}H and ^{13}C-NMR spectra, and electrospray mass spectra of rotaxanes and model compound

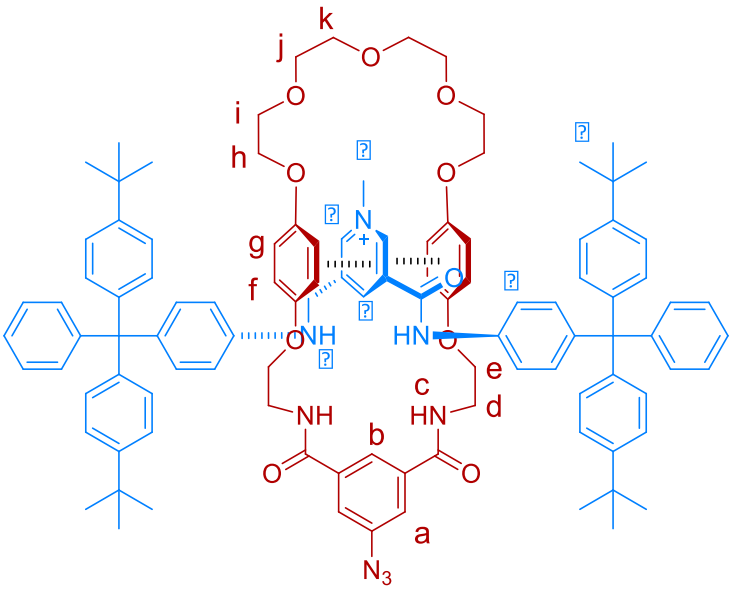

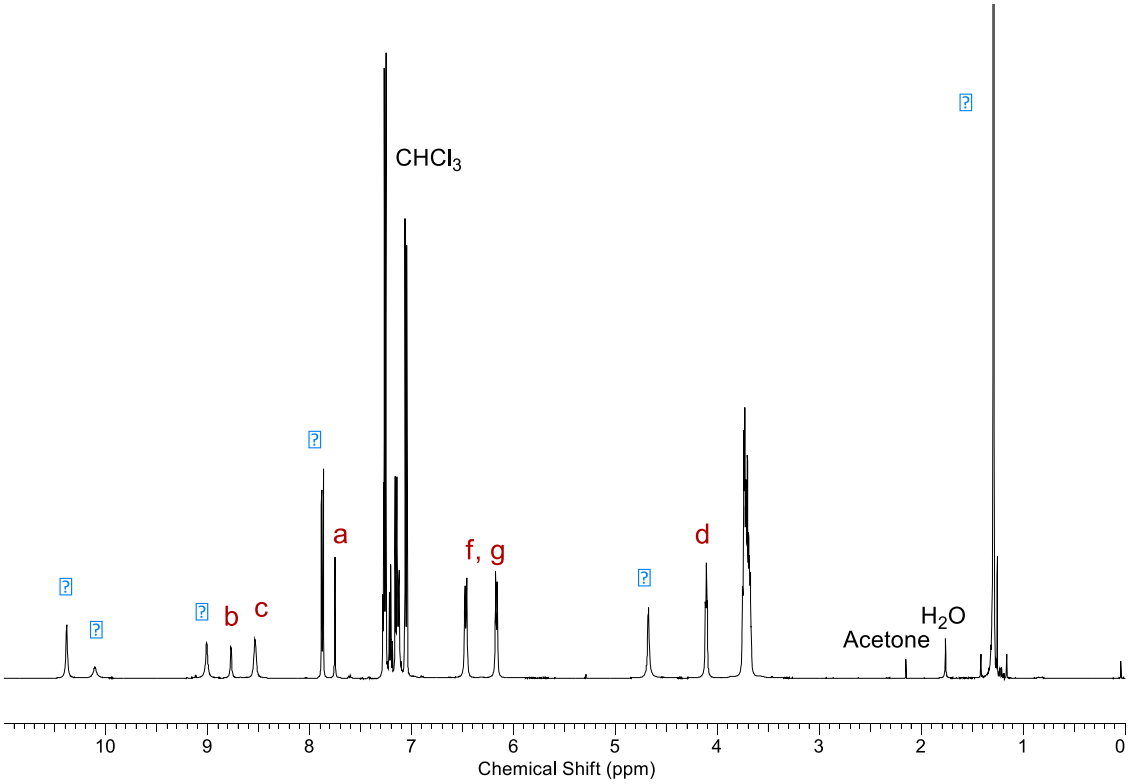

Figure S1: ^{1}H NMR spectrum of **4**·Cl ($CDCl_3$, 500MHz, 293 K).

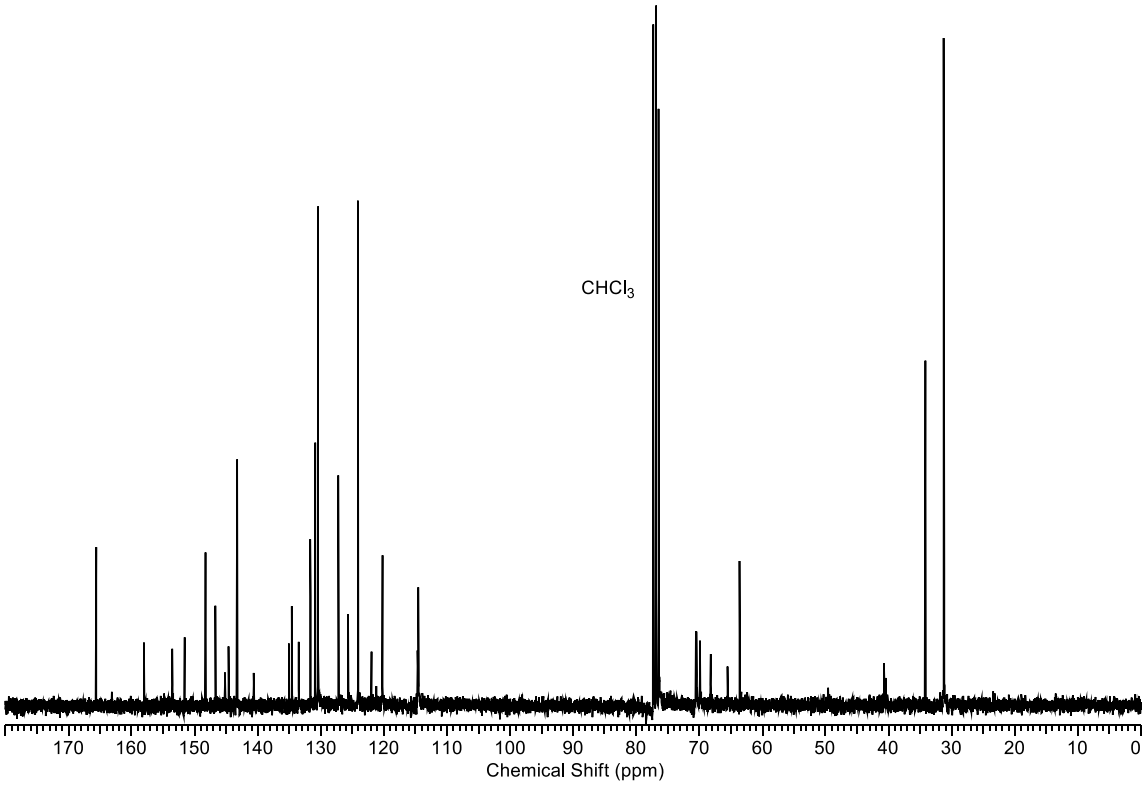

Figure S2: ^{13}C {^{1}H} NMR spectrum of **4**·Cl ($CDCl_3$, 75.5MHz, 293 K).

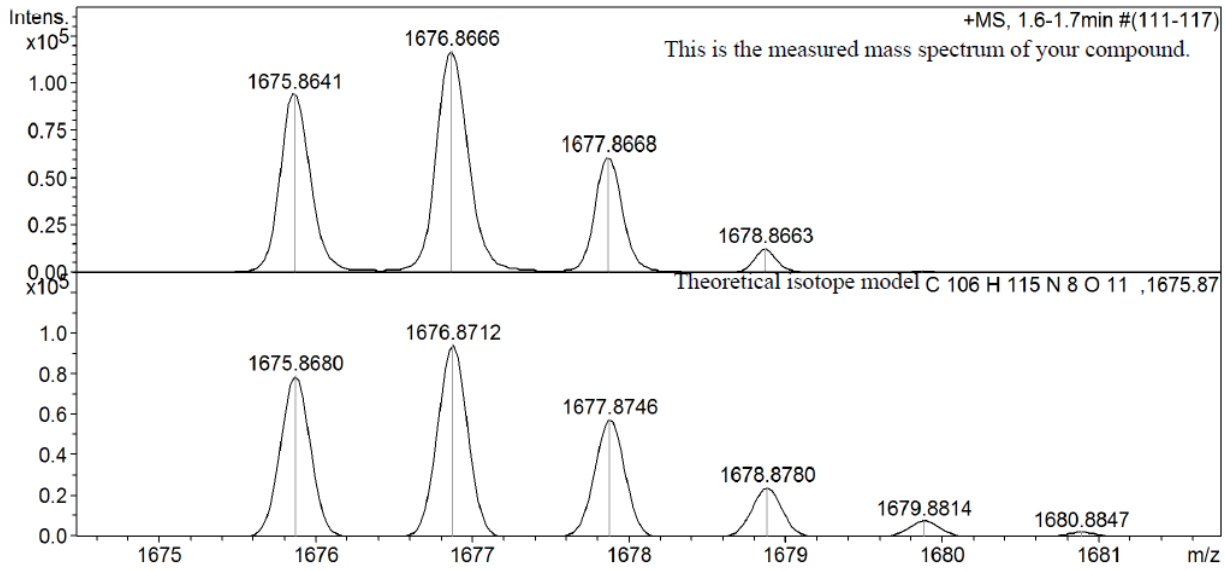

Figure S3: Electrospray mass spectrum of **4**·Cl (**top**) with theoretical isotope model for $[M–Cl]^+$ (**bottom**).

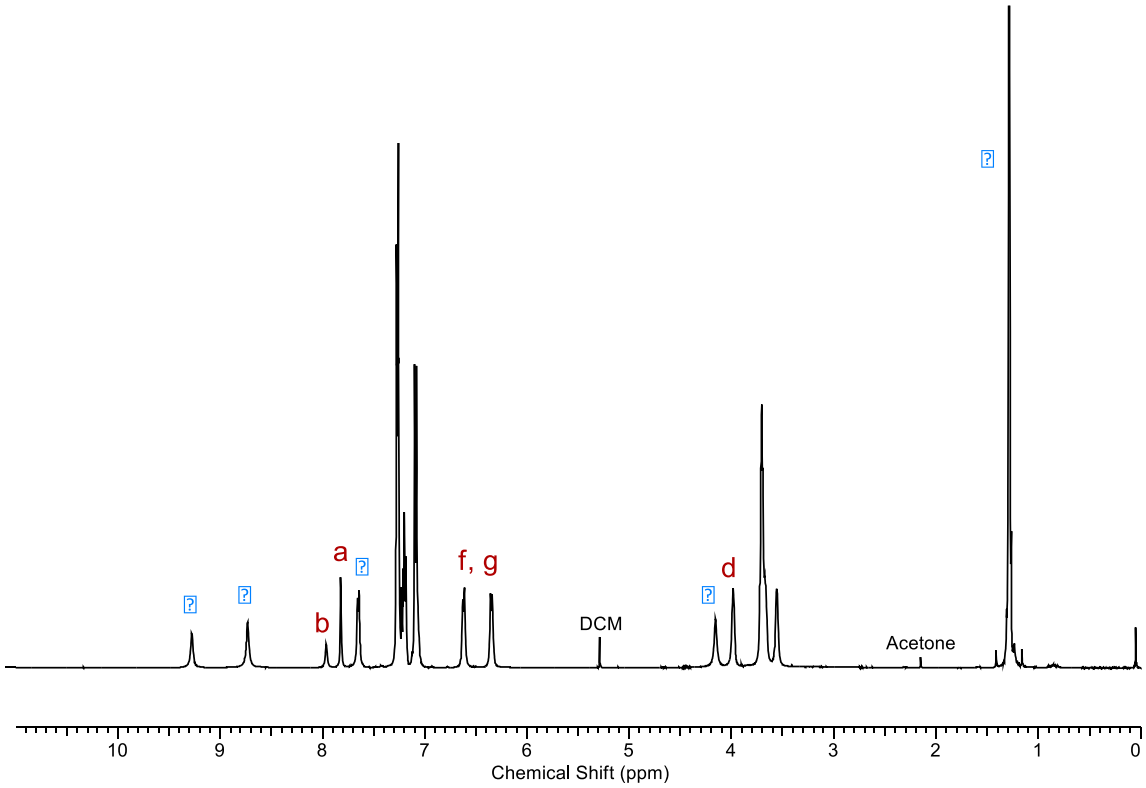

Figure S4: ^{1}H NMR spectrum of **4**·PF_6 ($CDCl_3$, 500MHz, 293 K).

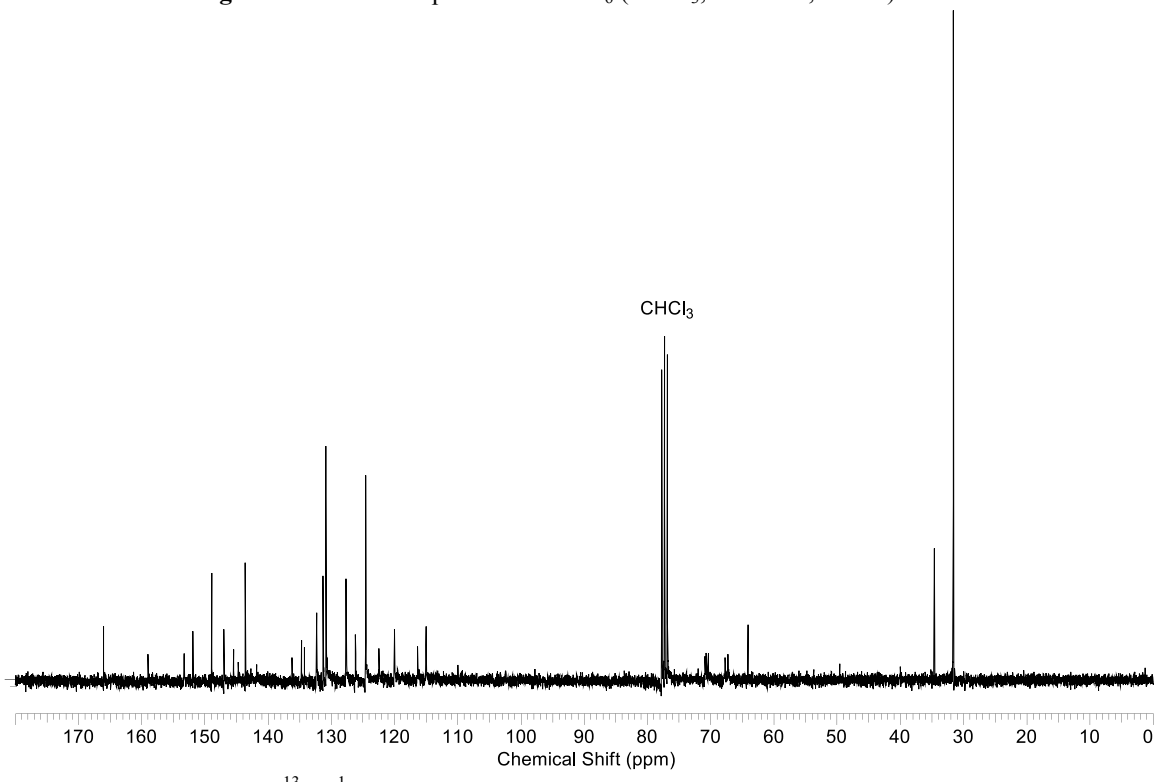

Figure S5: ^{13}C {^{1}H} NMR spectrum of **4**·PF_6 ($CDCl_3$, 75.5MHz, 293 K).

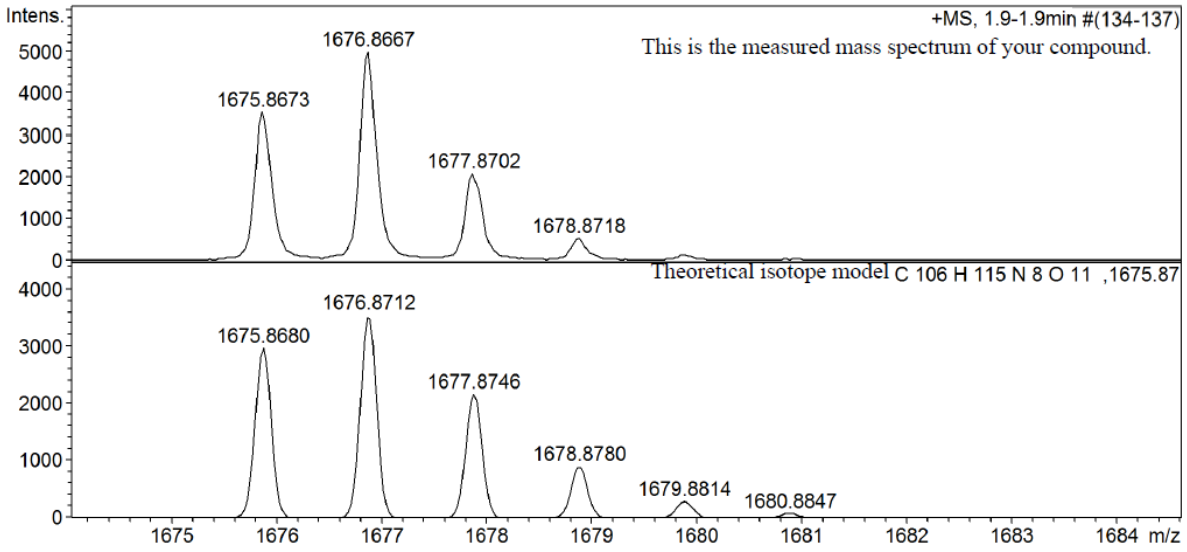

Figure S6: Electrospray mass spectrum of **4**·PF_6 (**top**) with theoretical isotope model for $[M–PF_6]^+$ (**bottom**).

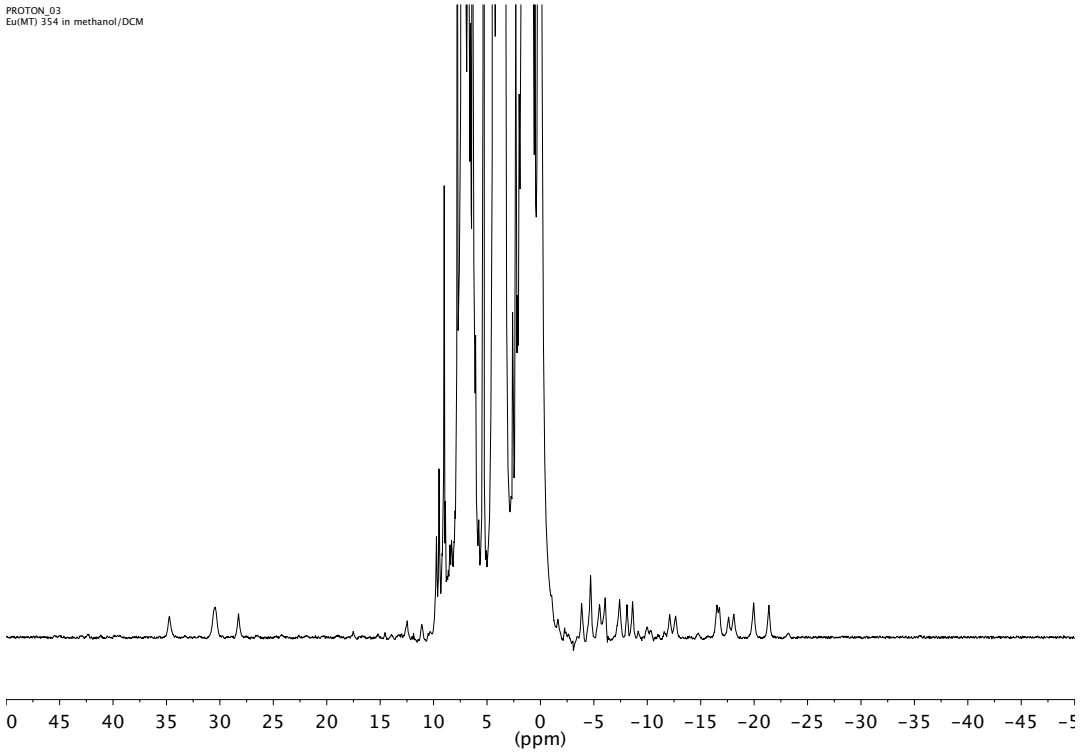

Figure S7. ^{1}H NMR spectrum of Eu·**1** (1:1 DCM/MeOH, 700MHz, 293 K).

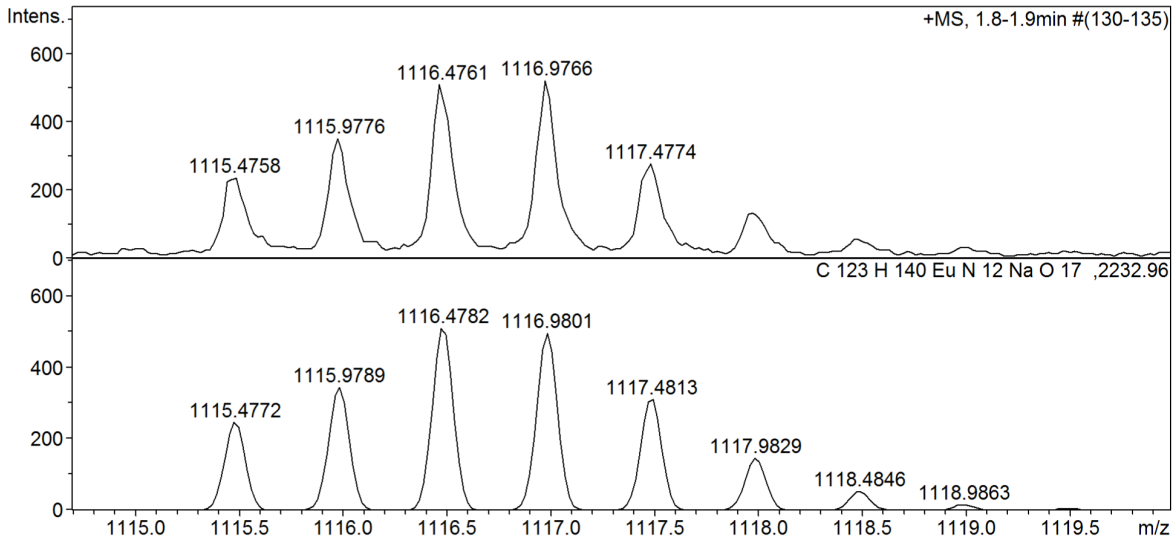

Figure S8: Electrospray mass spectrum of Eu·**1**·PF_6 (**top**) with theoretical isotope model for $[M–PF_6+ Na]^{2+}$ (**bottom**).

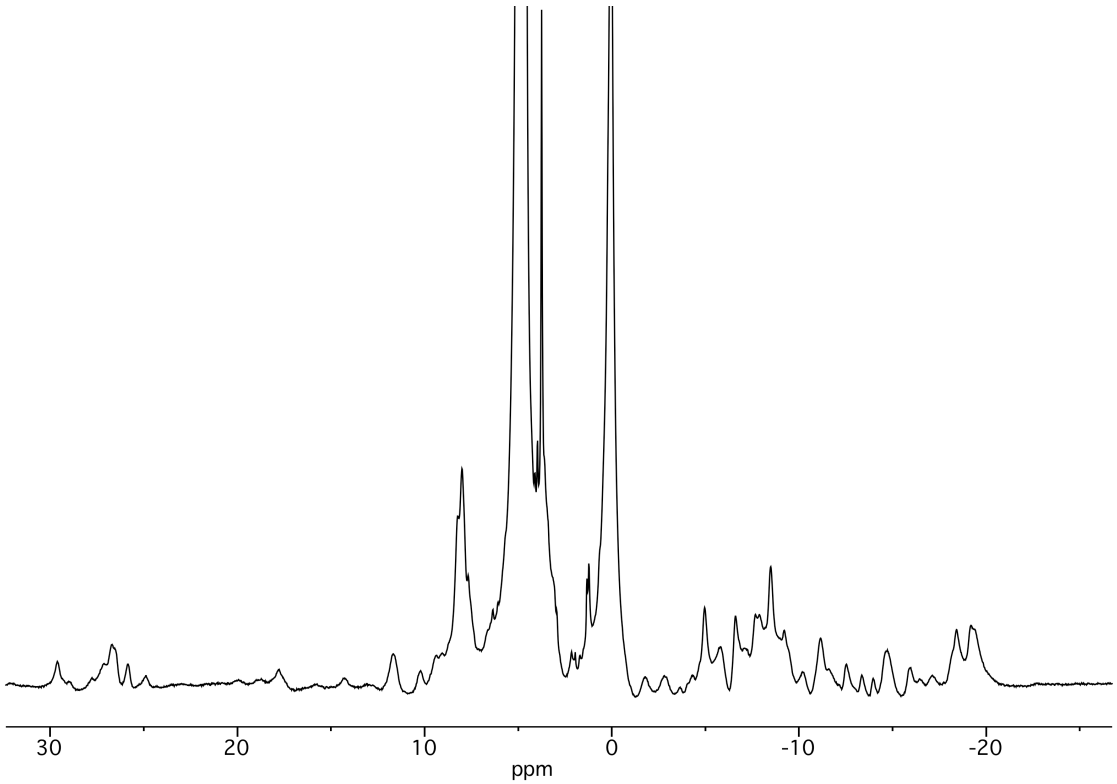

Figure S9. ^{1}H NMR spectrum of **6** (D_2O, 300MHz, 293 K).

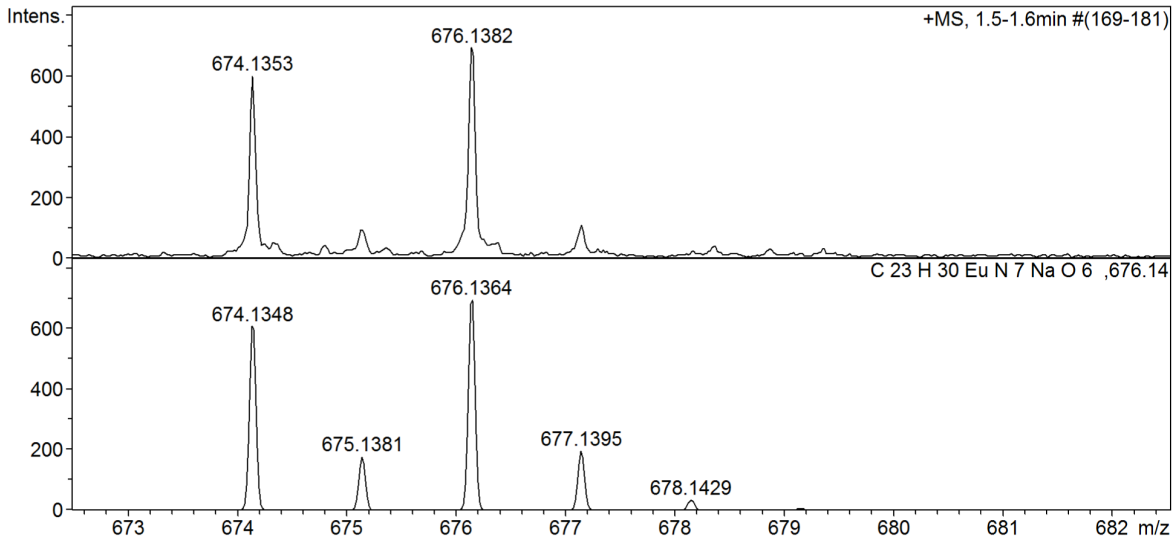

Figure S10: Electrospray mass spectrum of **6** (**top**) with theoretical isotope model for $[M+Na]^+$ (**bottom**).

Luminescence lifetime decays of rotaxanes and model compound

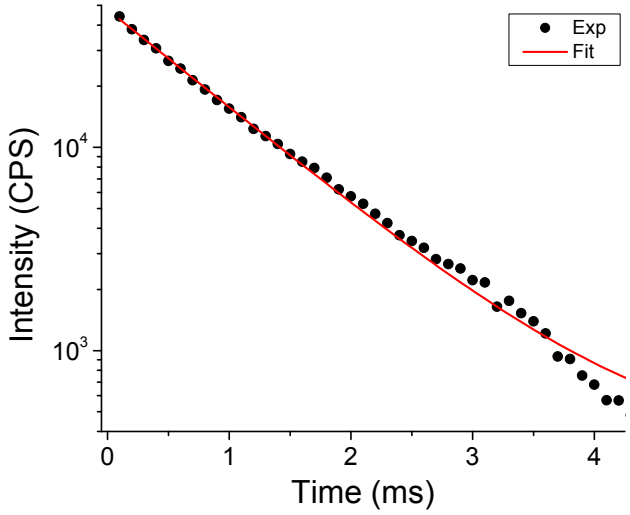

Figure S 11. Luminescence decay spectrum of Eu·**1** at 615 nm emission following excitation at 265 nm, in DCM.

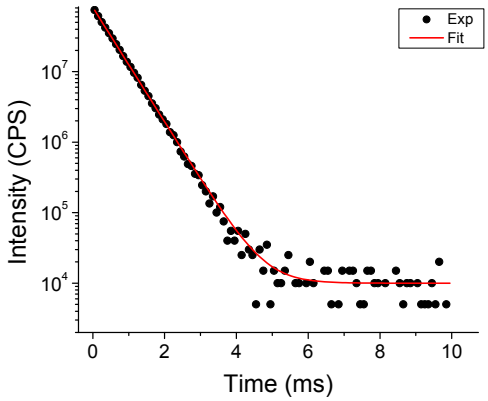

Figure S 12. Luminescence decay spectrum of **6** at 615 nm emission following excitation at 255 nm, in H_2O.

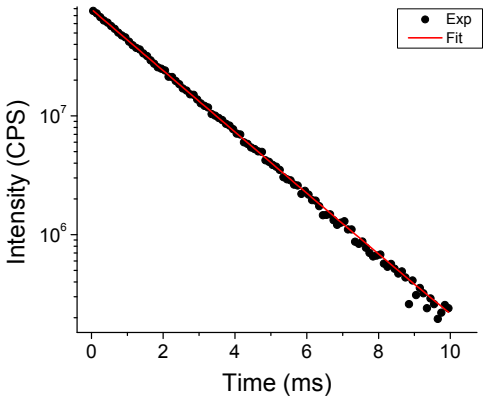

Figure S 13. Luminescence decay spectrum of **6** at 615 nm emission following excitation at 255 nm, in D_2O.

NMR Titrations

Protocol

^{1}H NMR spectra were recorded on a Varian Unity Plus 500 spectrometer. Typically, a solution of guest was added to a solution of the host at 293K. The chemical shift of the *internal* isophthalimide proton of the host was monitored for seventeen titration points (for 0, 0.2, 0.4, 0.6, 0.8, 1.0, 1.2, 1.4, 1.6, 1.8, 2.0, 2.5, 3.0, 4.0, 5.0, 7.0 and 10.0 equivalents of added guest). The resulting data were analysed using the WinEqNMR2[5] computer program in experiments where association of guest and host was fast on the NMR timescale. Anion binding titration experiments were carried out using the salt of the non-complexing tetrabutylammonium (TBA) cation as the guest species, titrated into the host species [2]rotaxanes **4**.PF_6 (in 45:45:10 $CDCl_3/CD_3OD/D_2O$). A 0.050 moldm^{-3} solution of anion was added to 0.5ml of a 0.002 mol dm^{-3}solution of [2]rotaxanes. The volumes of salt solution added were 10 × 4 μl, 2 × 10 μl, 2 × 20 μl, 1 × 40 μl, and 1 × 60 μl.

The values of the observed chemical shift and the guest concentration were entered into winEQNMR2 for every titration point, and estimates for the binding constant, limiting chemical shifts and binding stoichiometry made. The parameters were refined using non-linear least squares analysis to obtain the best fit between observed and calculated chemical shifts; the program plots the observed shift versus the guest concentration, revealing the accuracy of the experimental data and the suitability of the model used. The input parameters were varied until the best-fit values of the stability constants, together with their errors, converged.

Association Curves

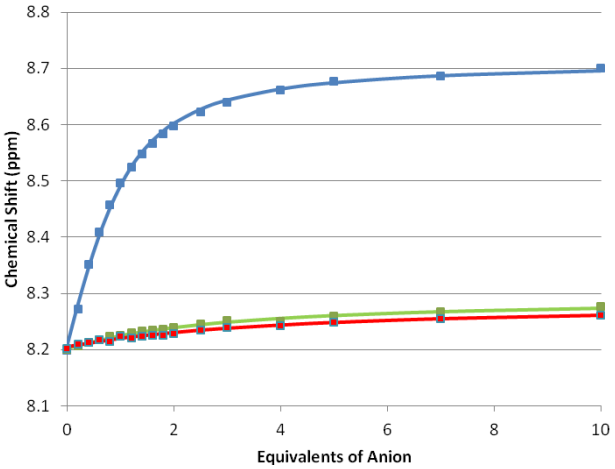

Anion	Binding Constant
Chloride	1464 (74)
Acetate	115 (21)
Dihydrogenphosphate	188 (28)

Figure S14: Change in chemical shift of proton *b* on addition of chloride (**blue**), acetate (**green**) and dihydrogenphosphate (**red**)**(left)** and calculated binding constants **(right)** of rotaxane **4**·PF_6 in $CHCl_3$/CD_3OD/D_2O (45:45:10) at 293K.

Crystal Structures

Data Experimental

Rotaxane **4**·Cl moiety Formula $C_{74}H_{78}N_3O_2$, $C_{32}H_{37}N_5O_9$, Cl; M = 1712.58; triclinic space group P -1; yellow; a = 13.2580(9) Å, b = 20.3837(18) Å, c = 26.4826(17) Å, α = 85.599(6)°, β = 81.344(5)°, γ = 81.232(6)°, V = 6982.0(9) Å^3; T = 100 K; μ = 0.07 mm^{-1}. 49935 reflections measured, 25858 independent (R_{int} = 0.140); final R = 0.133 (7598 reflections with $I > 2\sigma(I)$) and wR = 0.357; GooF = 1.15. Data were collected on the I19 beamline of the Diamond Light Source, Harwell, UK under an open flow of N_2 gas at 100 K.[6] Data were processed with the Crystal Clear Software package,[7] the structure solved with SIR92,[8] and refined on F_2 with CRYSTALS.[9] All non-hydrogen atoms were modeled with anisotropic displacement parameters, while hydrogen atoms were added geometrically and constrained in further refinement using a riding model. Vibrational, displacement and geometric restraints were applied where appropriate to ensure a physically reasonable model. A void of significant size containing highly disordered solvent was identified and modeled with SQUEEZE in PLATON (2788 Å^3 containing 280 electrons), approximating 2.5 diisopropyl ether molecules (290 electrons).[10]

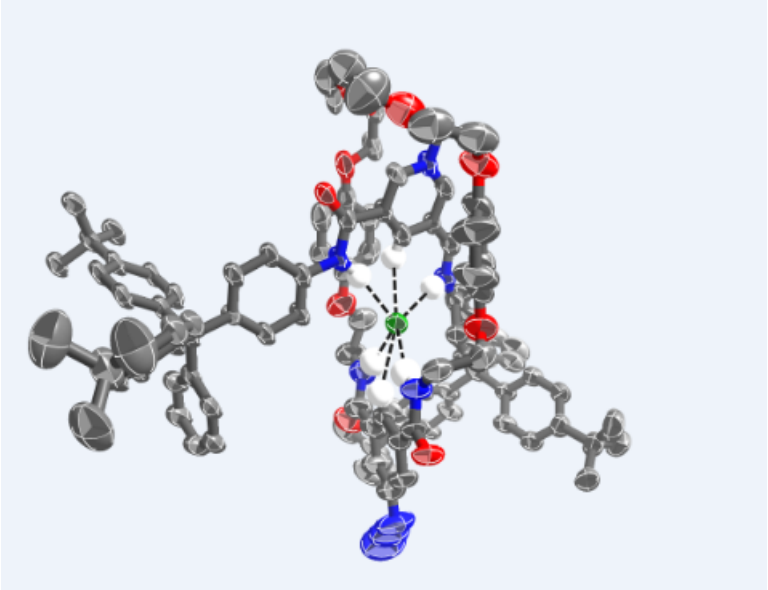

Figure S15. X-ray crystal structure of rotaxane **4**·Cl. Ellipsoids shown at 30% probability, non-protic hydrogen atoms omitted for clarity.

Lutetium complex Lu·**5** moiety Formula $C_{70}H_{102}Lu_4N_{16}Na_4O_{31}\cdot 12(H_2O)$; M = 2671.70; monoclinic space group P 2/c; colourless; a = 18.0616(2) Å, b = 14.9090(2) Å, c = 18.2262(3) Å, α = 90°, β = 108.6904(8)°, γ = 90°, V = 4667.84(11) Å^3; T = 150 K; μ = 4.313 mm^{-1}. 84881 reflections measured, 10639 independent (R_{int} = 0.0402); final R = 0.064 (9306 reflections with $I > 2\sigma(I)$) and wR = 0.168; GooF = 0.994. **A** crystal was mounted using the oil drop technique, in perfluoropolyether oil at 150(2) K using a Cryostream N_2 open-flow cooling device.(Cosier, J.; Glazer, A. M. *Journal of Applied Crystallography* **1986,** *19*, 105) Diffraction data were collected using graphite monochromatic Mo-K$_\alpha$ radiation (λ = 0.71073 Å) on a Nonius Kappa CCD diffractometer. A series of ω-scans was performed in such a way as to collect a complete data set to a maximum resolution of 0.77 Å. Data reduction including unit cell refinement and inter-frame scaling was carried out using DENZO-SMN/SCALEPACK.(Otwinowski, Z.; Minor, W. *Macromolecular Crystallography, Pt A* **1997,** *276*, 307) Intensity data were processed and corrected for absorption effects by the multi-scan method, based on repeat measurements of identical and Laue equivalent reflections. Structure solution was carried out with direct methods using the program SIR92(Altomare, A.; Cascarano, G.; Giacovazzo, C.; Guagliardi, A. *Journal of Applied Crystallography* **1994,** *27*, 104) within the CRYSTALS software suite.(Watkin, D.; Cooper, R.; Prout, C. K. *Zeitschrift Fur Kristallographie* **2002,** *217*, 429) In general, coordinates and anisotropic displacement parameters of all non-hydrogen atoms were refined freely except where disorder necessitated the use of "same distance restraints" together with thermal similarity and vibrational restraints to maintain sensible geometry/displacement parameters. Hydrogen atoms were generally visible in the difference map and refined with soft restraints prior to inclusion in the final refinement using a riding model.(Cooper, R. I.; Thompson, A. L.; Watkin, D. J. *Journal of Applied Crystallography* **2010,** *43*, 1100)

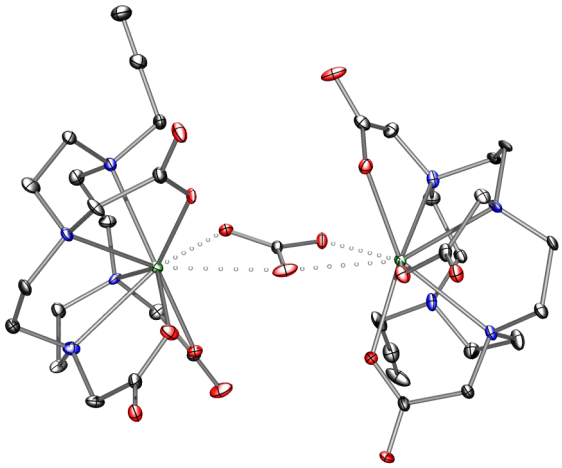

Figure S15. Ortep depiction of the X-ray crystal structure of Lu·**5**. Ellipsoids are shown at 30% probability with the hydrogen atoms, sodium ions and water omitted for clarity.

Fluorescence binding studies

Structures of the rotaxane and model compound

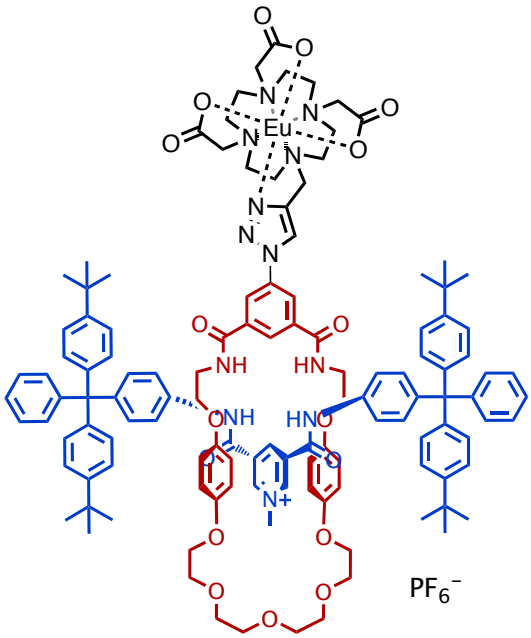

Eu.1

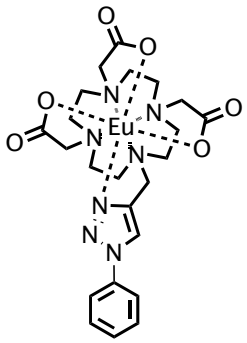

6

Figure S16. Molecular structures of the europium-containing rotaxane with europium and pyridinium binding pockets **Eu·1** and europium binding pocket model compound **6** investigated in this study.

Equilibria

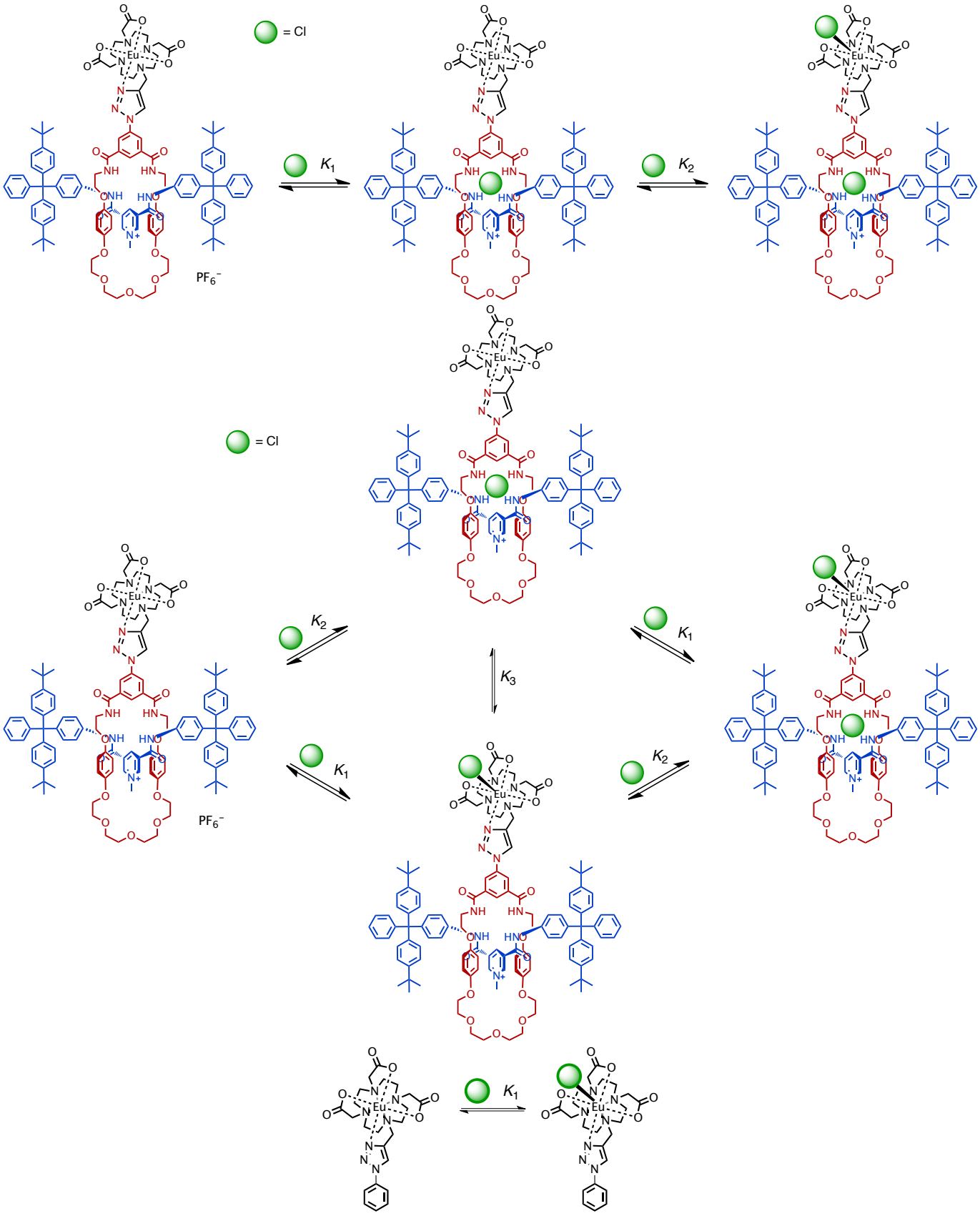

Figure S17. Anion binding equilibria proposed for the europium-containing rotaxane and model compound in the case of chloride in dichloromethane.

Fitting using Dynafit

Dynafit was used to fit the responses observed in the luminescence spectrum of the Eu complexes upon addition of anion to the solution. As the dilution method was used for the titrations, the concentration independent intensity ratio was used to determine the association constant. If intensities had to be used, only data obtained with a dilution of less than 5% were employed.
As the binding behavior in most cases a simple 1:1 binding, the advanced capabilities of Dynafit were not used. The script used to determine all the association constants is given below.

Example of Dynafit script

```
[task]

  data = equilibra
  task = fit

[mechanism]
  Eurotaxane + Cl  <==> Eurotaxane.Cl     :  K1 assoc

[constants]

  K1 = 100000 ??

[concentrations]

 Eurotaxane = 3.916e-005

[equilibria]
variable  Cl

file C:\Users\Manuel\Desktop\Eu_rotaxane\MT354_DCM\Dynafit_input\MT354_DCM_Cl_DJ=2_DJ1.txt | response
Eurotaxane=15490 ?, Eurotaxane.Cl=30000 ?
file C:\Users\Manuel\Desktop\Eu_rotaxane\MT354_DCM\Dynafit_input\MT354_DCM_Cl_DJ=2_DJ4.txt |response
Eurotaxane=16480 ?, Eurotaxane.Cl=30000 ?
;file C:\Users\Manuel\Desktop\Eu_rotaxane\MT354_DCM\Dynafit_input\MT354_DCM_Cl_DJ=2_DJ0.txt |response
Eurotaxane=16480 ?, Eurotaxane.Cl=30000

[output]
  directory C:\Users\Manuel\Desktop\Eu_rotaxane\MT354_DCM\Dynafit_output\MT354_DCM_Cl_DJ_ratios_all\

[end]
```

Modeling of the binding of chloride by the Eu rotaxane Eu.1 in dichloromethane

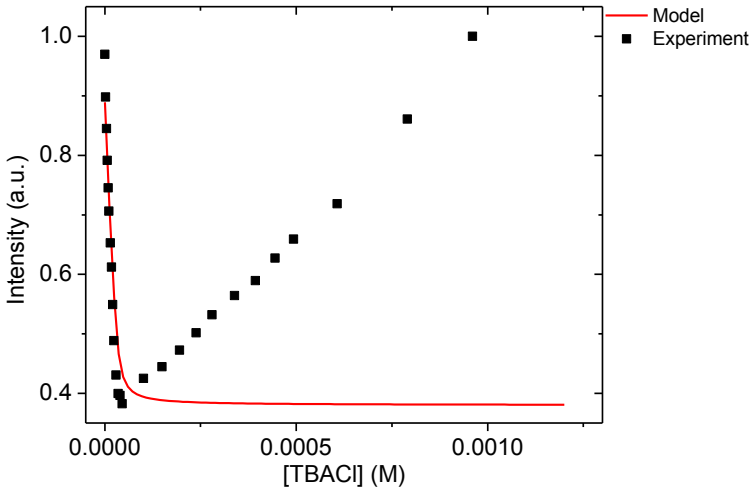

Figure S18. Eu rotaxane titrated with TBACl in DCM. The experimental data (squares, *ΔJ=2*) are modeled to a 1:1 binding event with an association constant of $K_1 = 505000\ M^{-1}$.

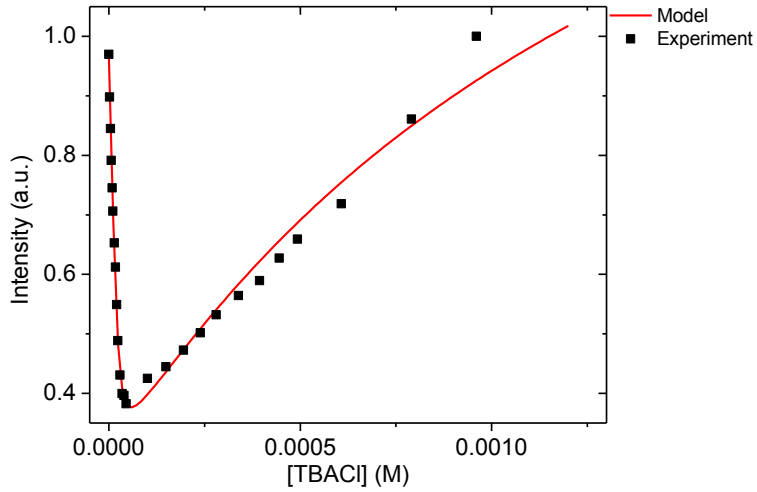

Figure S19. Eu rotaxane titrated with TBACl in DCM. The experimental data (squares, *ΔJ=2*) are modeled (full line) to two sequential 1:1 binding events between the Eu-rotaxane and chloride with association constants of $K_1 = 505000\ M^{-1}$ and $K_2 = 625\ M^{-1}$.

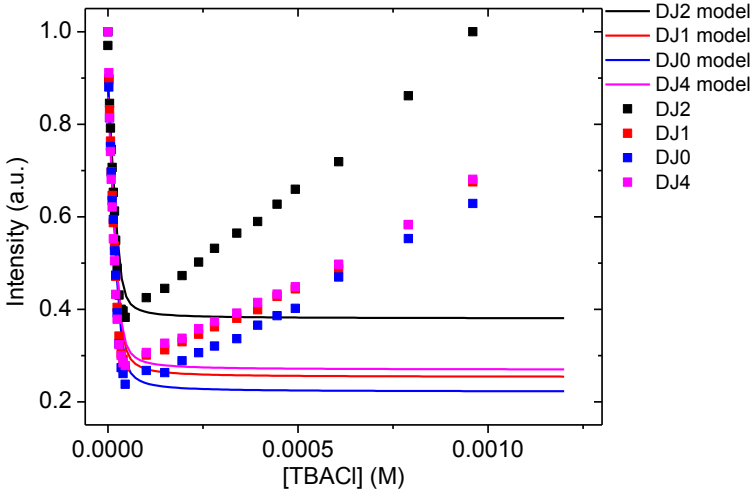

Figure S20. Eu rotaxane titrated with TBACl in DCM. The experimental data (squares) are modeled (full line) to a 1:1 binding event with an association constant of $K_1 = 505000\ M^{-1}$.

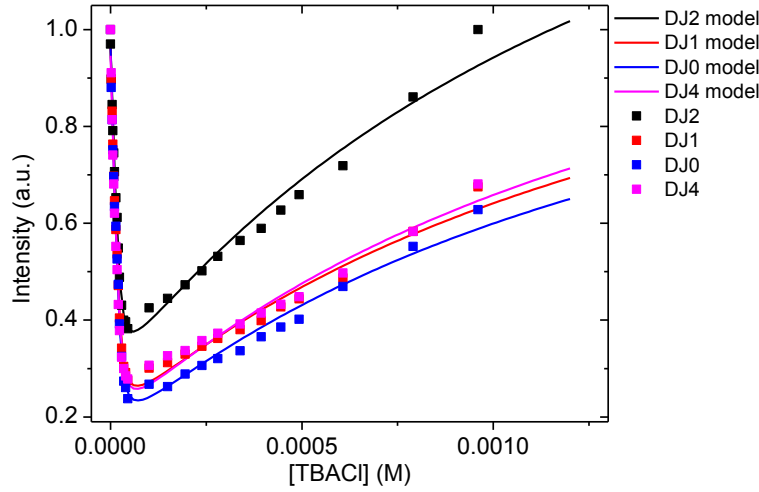

Figure S21. Eu rotaxane titrated with TBACl in DCM. The experimental data (squares) are modeled (full line) to two sequential 1:1 binding events between the Eu-rotaxane and chloride with association constants of $K_1 = 505000\ M^{-1}$ and $K_2 = 625\ M^{-1}$.

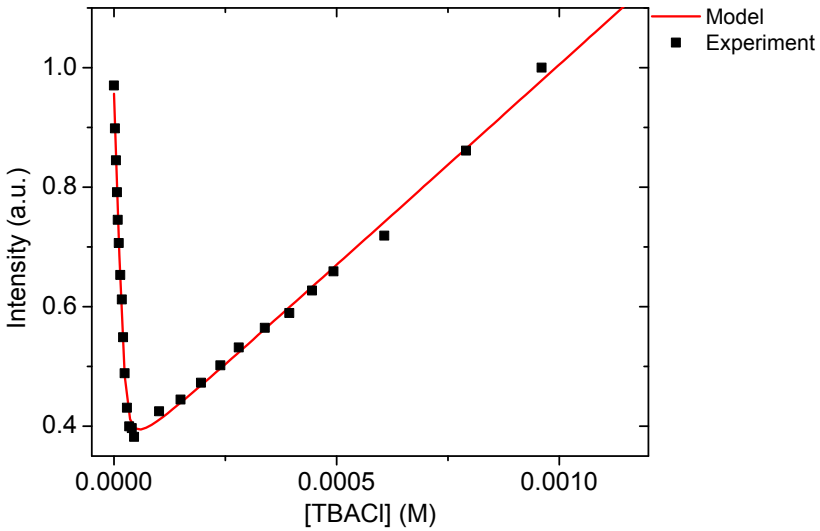

Figure S 22. Eu rotaxane titrated with TBACl in DCM. The experimental data (squares, *ΔJ=2*) are modeled (full line) to two independent 1:1 binding events between the Eu-rotaxane and chloride with association constants of K_1 = 750000 M^{-1}, K_2 = 1360 M^{-1} and K_3 = 550.

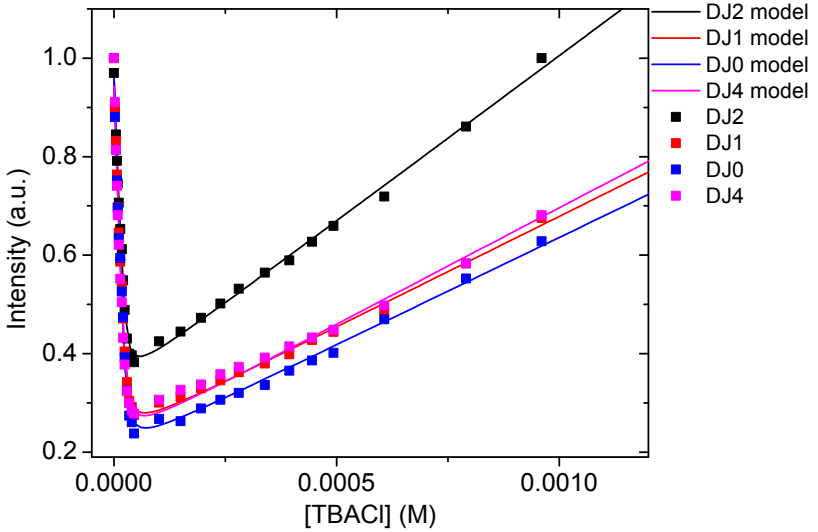

Figure S 23. Eu rotaxane titrated with TBACl in DCM. The experimental data (squares) are modeled (full line) to two independent 1:1 binding events between the Eu-rotaxane and chloride with association constants of K_1 = 750000 M^{-1}, K_2 = 1360 M^{-1} and K_3 = 550.

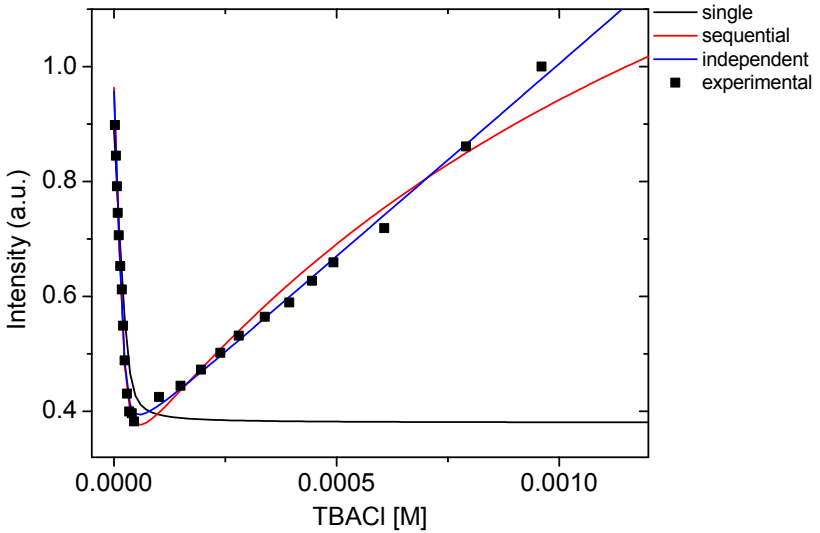

Figure S 24. Eu rotaxane titrated with TBACl in DCM. Overlay of the 1:1 single binding event model with the models representing two sequential and independent 1:1 binding events (full line) and the experimental data (squares, *ΔJ=2*).

Binding of anions by the Eu rotaxane Eu·4 in dichloromethane - spectra

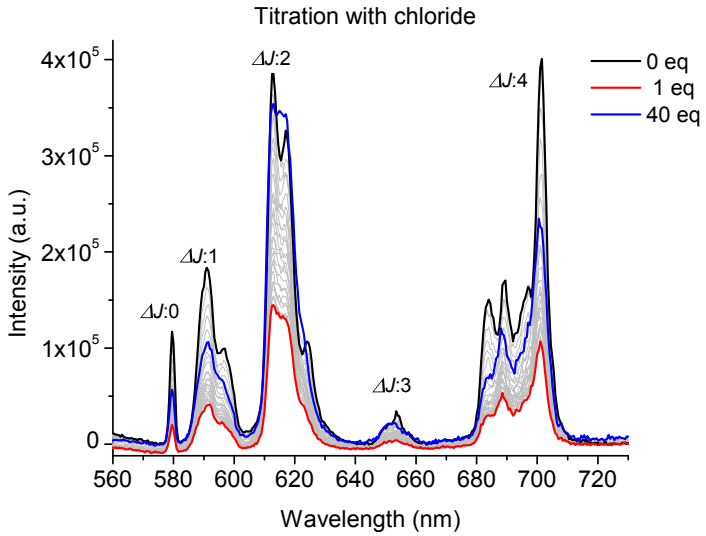

Figure S25. Changes in Eu-centred emission of the Eu-rotaxane (10^{-5}M, DCM) upon addition of TBACl (0 to 40 equivalents) with 265 nm excitation.

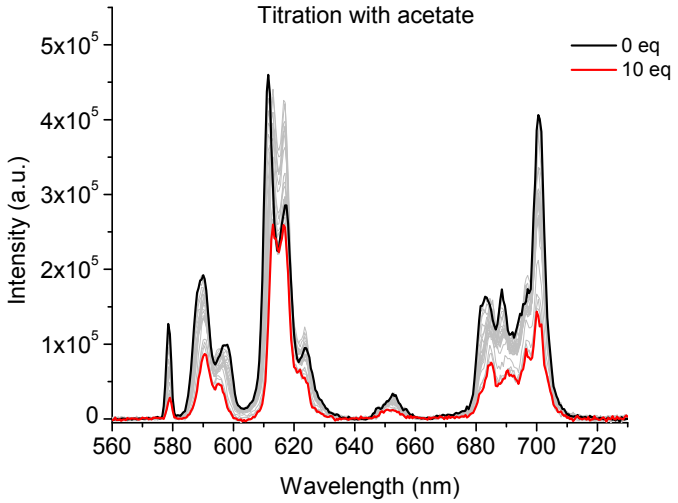

Figure S26. Changes in Eu-centred emission of the Eu-rotaxane (10^{-5}M, DCM) upon addition of TBAOAc (0 to 10 equivalents) with 265 nm excitation.

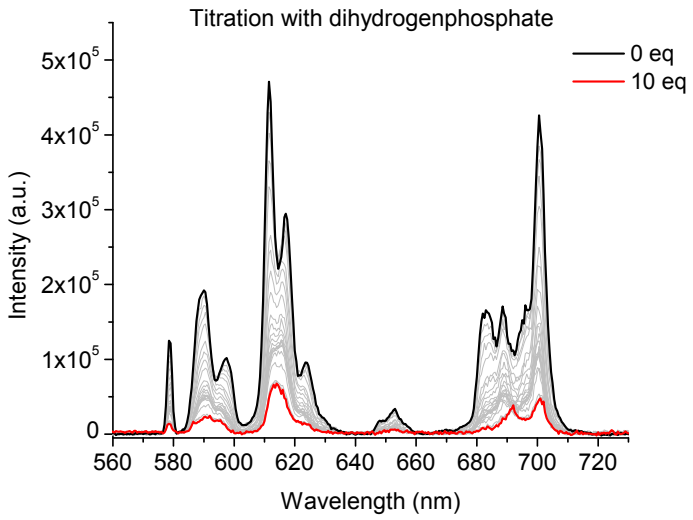

Figure S27. Changes in Eu-centred emission of the Eu-rotaxane (10^{-5}M, DCM) upon addition of $TBAH_2PO_4$ (0 to 10 equivalents) with 265 nm excitation.

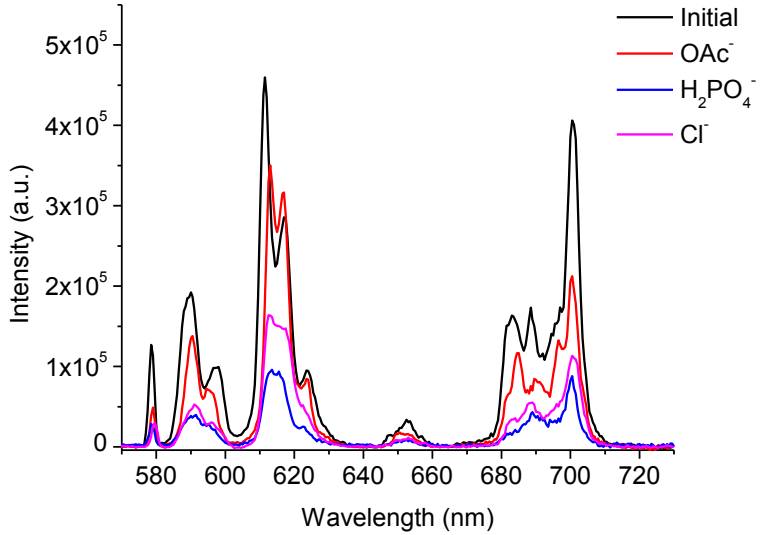

Figure S28. Overlay of the changes in Eu-centred emission of Eu-rotaxane upon addition of chloride (2 eq.), acetate and dihydrogenphosphate (3 eq.).

Binding of anions by the Eu rotaxane Eu·1 in dichloromethane – intensity

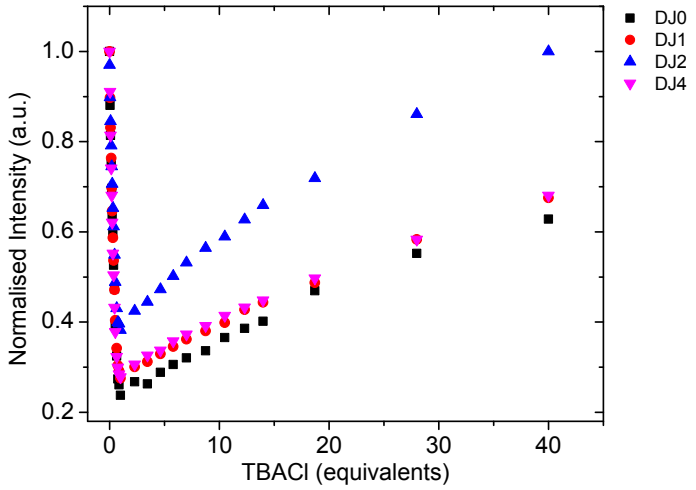

Figure S29. Titration of a 10^{-5}M solution of the Eu-rotaxane with TBACl (10^{-3}M) in DCM followed monitoring the four most intense Eu centred transition with 265 nm excitation.

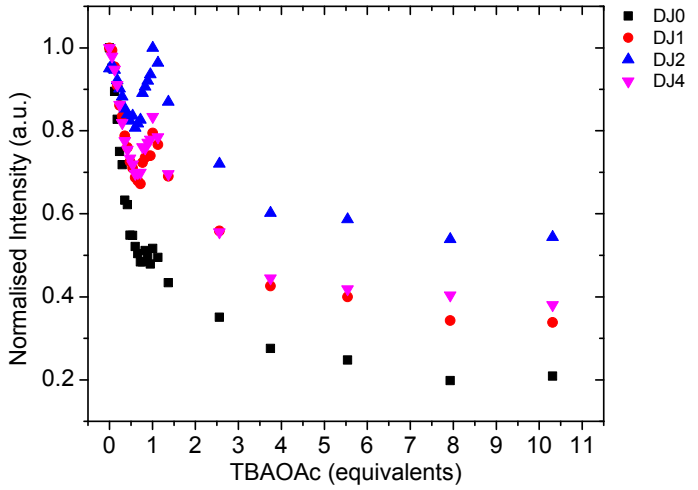

Figure S30. Titration of a 10^{-5}M solution of Eu-rotaxane with TBAOAc (10^{-3}M) in DCM followed monitoring the four most intense Eu centred transition with 265 nm excitation.

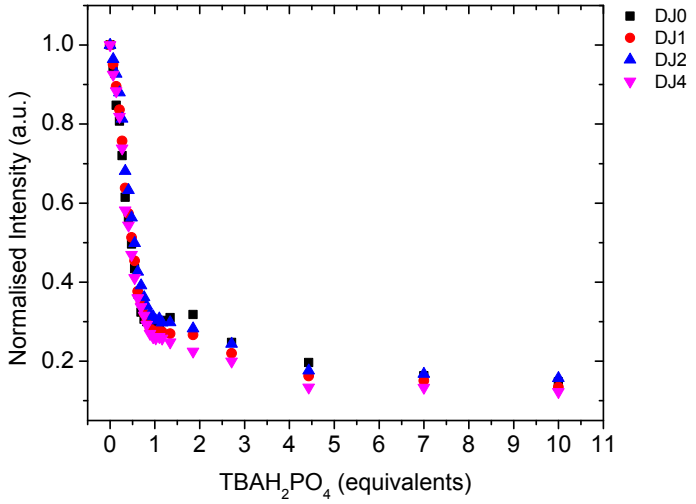

Figure S31. Titration of a 10^{-5}M solution of Eu-rotaxane with $TBAH_2PO_4$ (10^{-3}M) in DCM followed monitoring the four most intense Eu centred transition under 265 nm excitation.

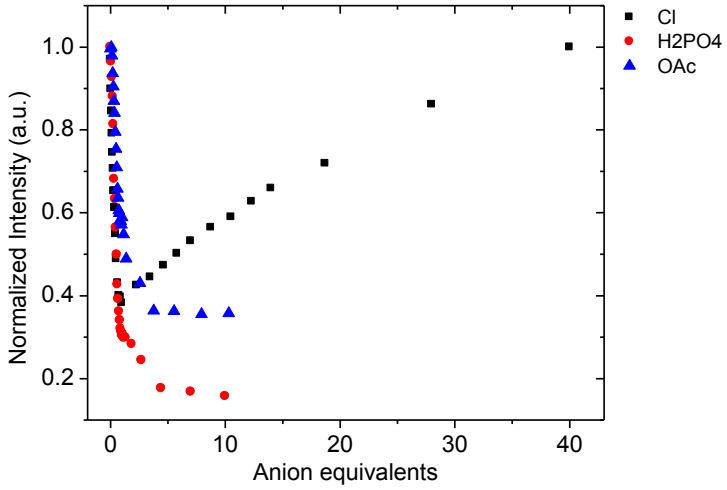

Figure S32. Comparison of a 10^{-5}M solution of Eu-rotaxane ΔJ=2 emission upon addition of chloride, acetate and dihydrogenphosphate (10^{-3}M) in DCM.

Binding of anions by the Eu rotaxane Eu·1 in dichloromethane – the hypersensitive ΔJ=2 transition

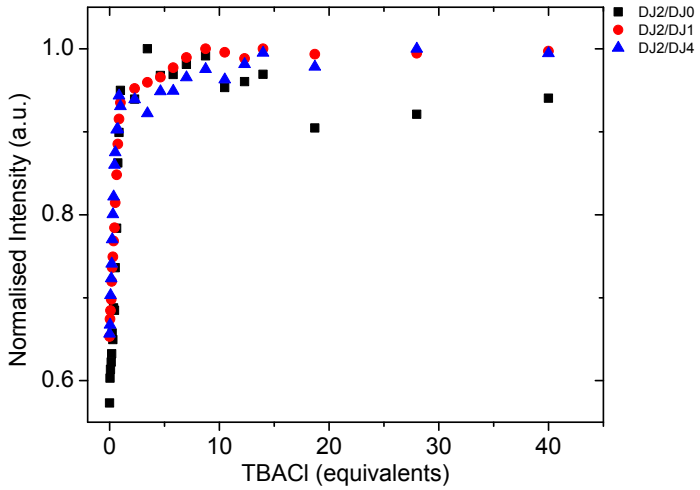

Figure S33. Titration of a 10^{-5}M solution of Eu-rotaxane with TBACl (10^{-3}M) in DCM followed monitoring the intensity ratio of Eu centred transitions with 265 nm excitation.

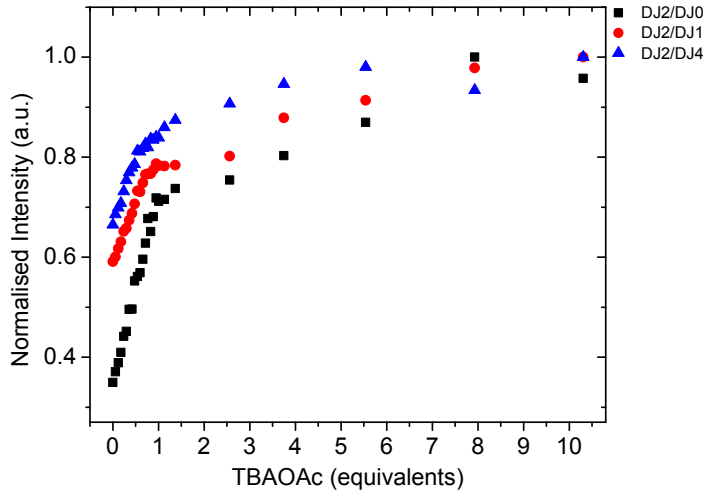

Figure S34. Titration of a 10^{-5}M solution of Eu-rotaxane with TBAOAc (10^{-3}M) in DCM followed monitoring the intensity ratio of Eu centred transitions with 265 nm excitation.

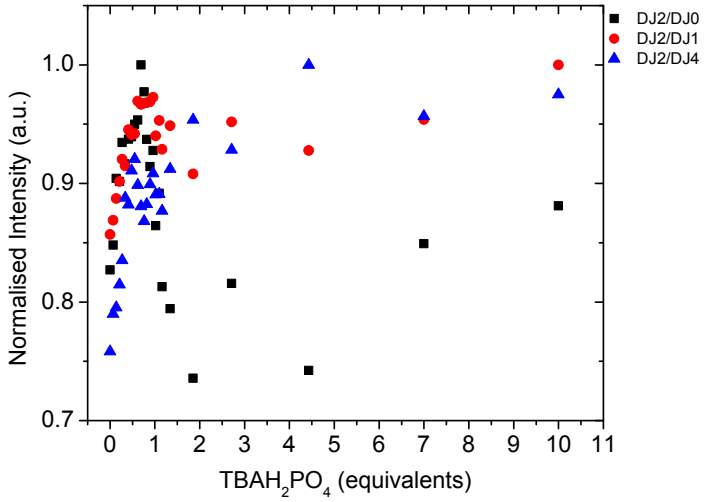

Figure S35. Titration of a 10^{-5}M solution of Eu-rotaxane with $TBAH_2PO_4$ (10^{-3}M) in DCM followed monitoring the intensity ratio of Eu centred transitions with 265 nm excitation.

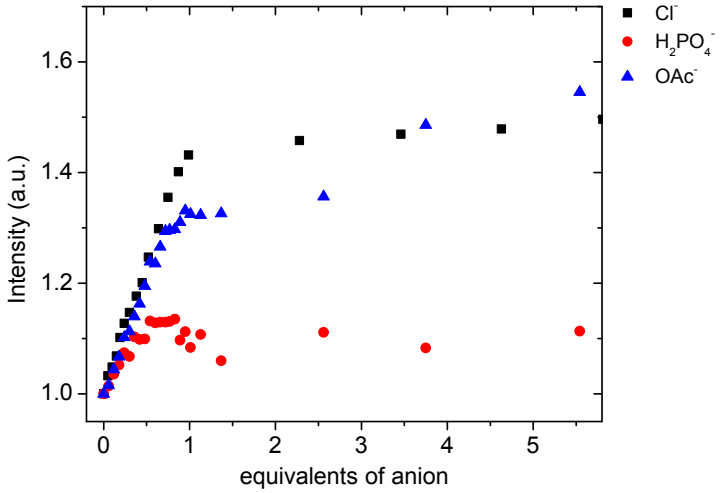

Figure S36. Comparison of the *ΔJ2/ΔJ1* intensity ratios of a 10^{-5}M solution of Eu-rotaxane upon addition of chloride, acetate and dihydrogenphosphate (10^{-3}M) in DCM.

Binding of chloride by the Eu rotaxane Eu·1 in dichloromethane - lifetimes

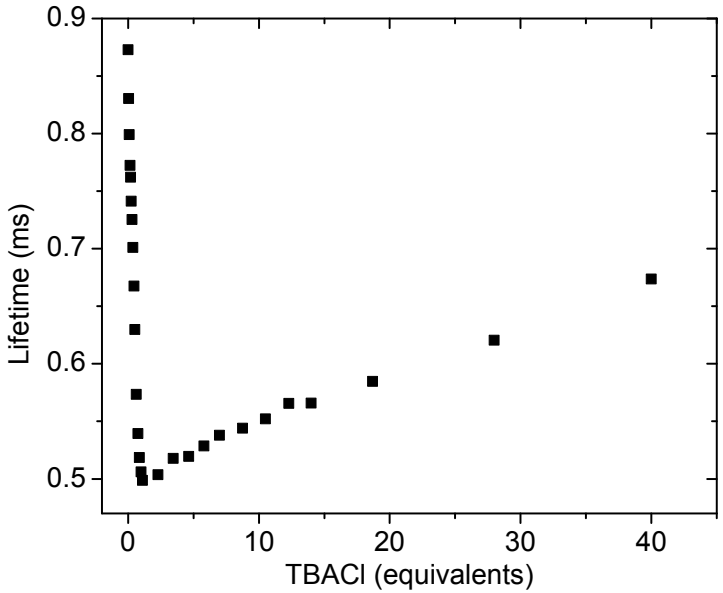

Figure S37. Titration of a 10^{-5}M solution of Eu-rotaxane with TBACl (10^{-3}M) in DCM followed monitoring the lifetime of the ΔJ=2 transition upon 265 nm excitation.

Table S1. Representative values of luminescence lifetime of the ΔJ=2 transition of a 10^{-5} M solution of Eu.1 upon addition of TBACl (10^{-3} M) in DCM with 265 nm excitation.

equivalents of chloride	lifetime (ms)
0	0.85
1	0.49
40	0.64

Binding of anions by the Eu rotaxane Eu.1 in dichloromethane – Dynafit results

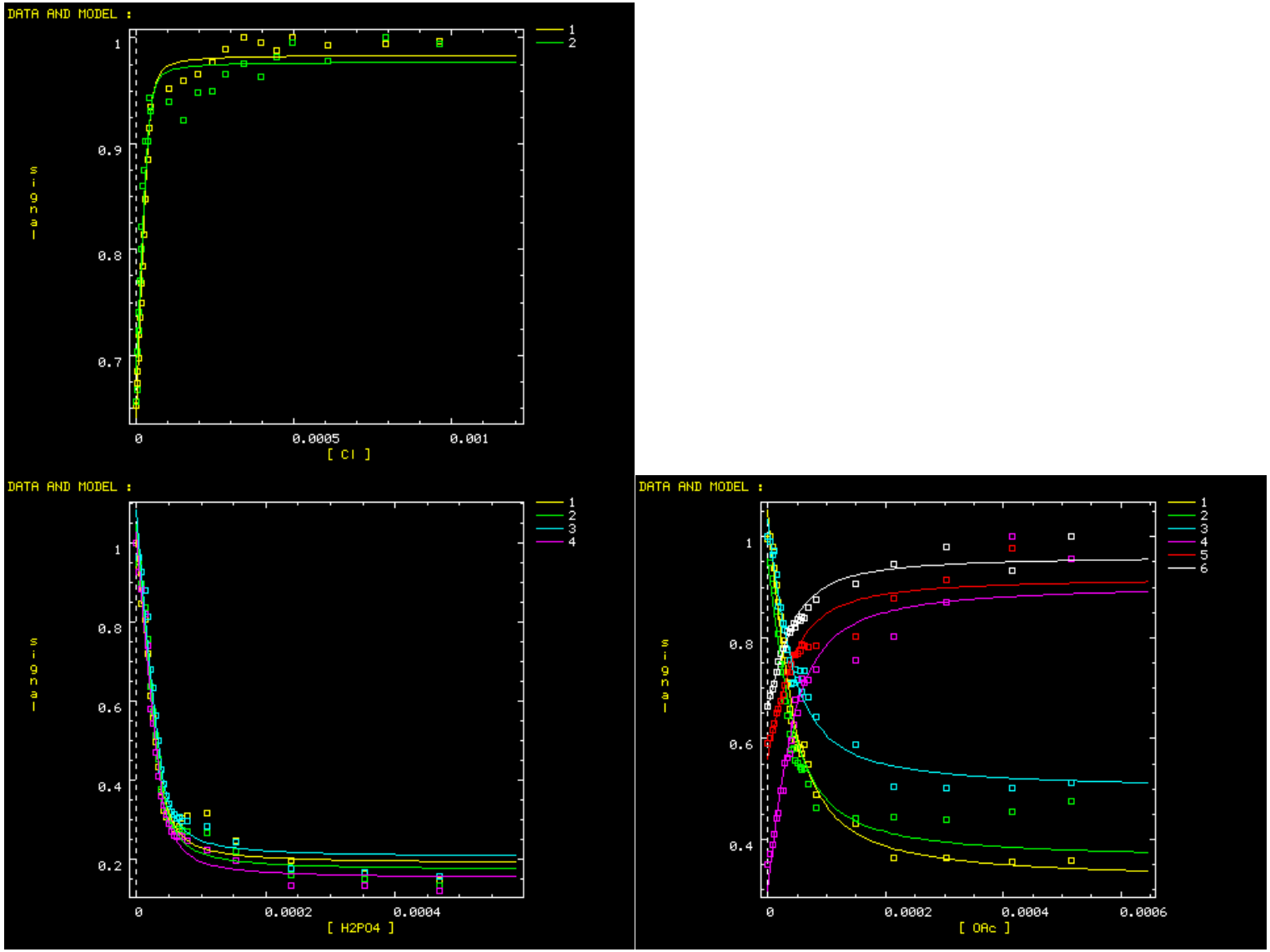

Figure S38. Dynafit output for the titration of Eu-rotaxane with chloride, acetate and dihydrogenphosphate in DCM. Data (squares) are intensities of the emission signal and/or the intensity ratio (ΔJ=2/ΔJ=N) upon addition of anion for several europium transitions, while fits (lines) are obtained using a 1:1 binding model.

Binding of anions by the Eu rotaxane Eu·1 in 1:1 dichloromethane/methanol - spectra

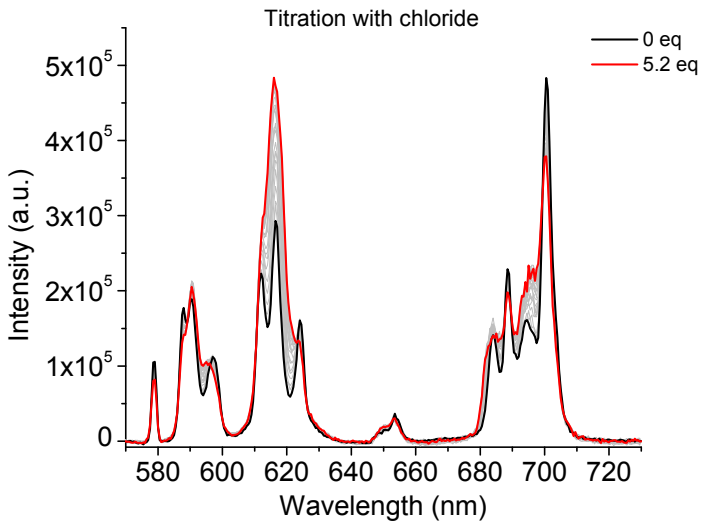

Figure S39. Changes in Eu-centred emission of Eu-rotaxane (10^{-5} M, 1:1 DCM/MeOH) upon addition of TBACl (0 to 5 equivalents) with 265 nm excitation.

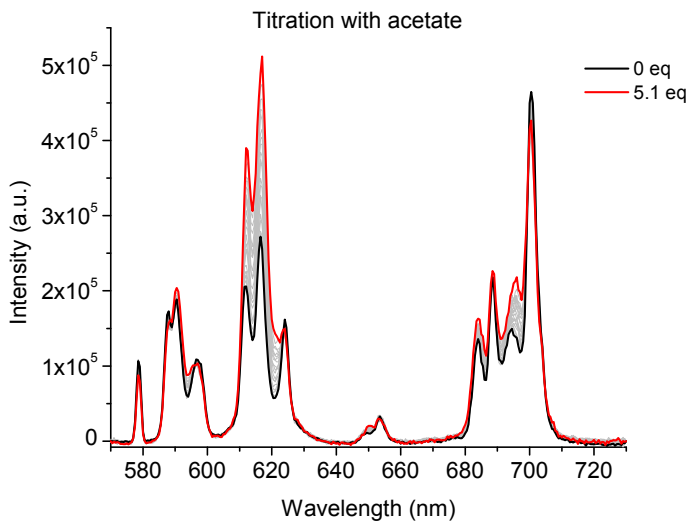

Figure S40. Changes in Eu-centred emission of Eu-rotaxane (10^{-5} M, 1:1 DCM/MeOH) upon addition of TBAOAc (0 to 5 equivalents) with 265 nm excitation.

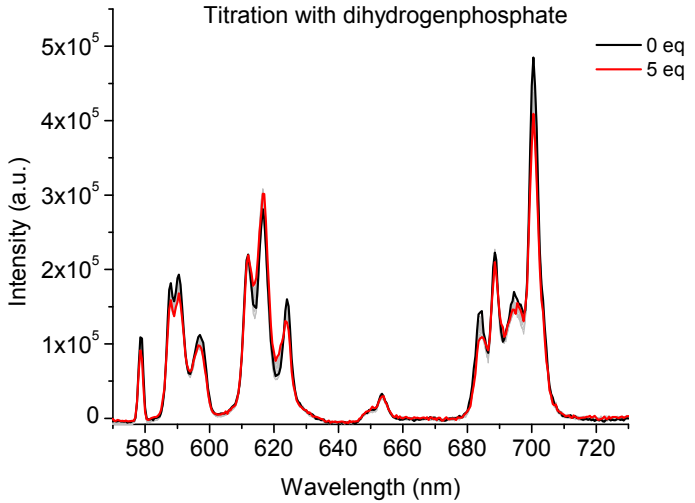

Figure S41. Changes in Eu-centred emission of Eu-rotaxane (10^{-5} M, 1:1 DCM/MeOH) upon addition of $TBAH_2PO_4$ (0 to 5 equivalents) with 265 nm excitation.

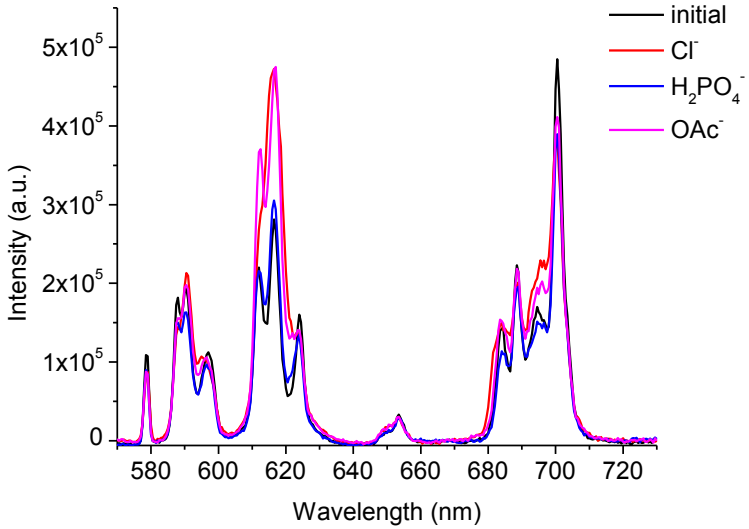

Figure S42. Overlay of the changes in Eu-centred emission of Eu-rotaxane upon addition of chloride (2 eq.), acetate and hydrogenphosphate (3 eq.) in 1:1 DCM/MeOH.

Binding of anions by the Eu rotaxane Eu·1 in 1:1 dichloromethane/methanol - intensity

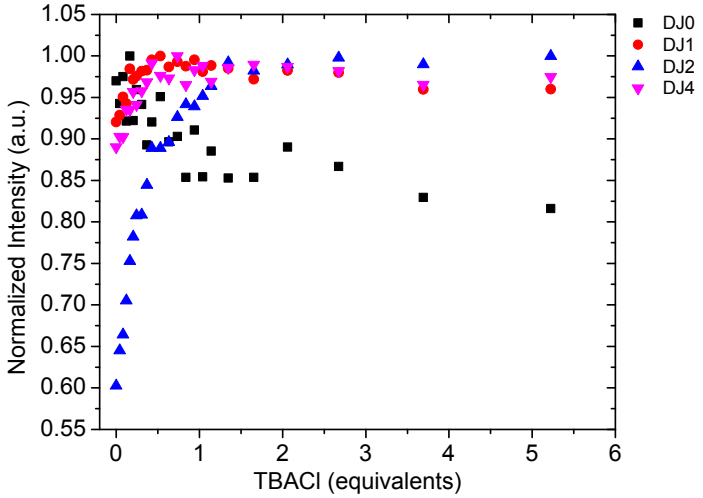

Figure S43. Titration of a 10^{-5}M solution of Eu-rotaxane with TBACl (10^{-3}M) in 1:1 DCM/MeOH followed monitoring the four most intense Eu centred transitions with 265 nm excitation.

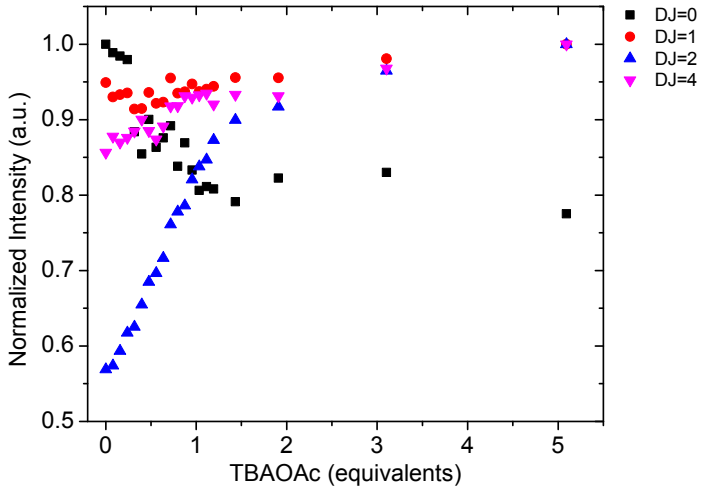

Figure S44. Titration of a 10^{-5}M solution of Eu-rotaxane with TBAOAc (10^{-3}M) in 1:1 DCM/MeOH followed by monitoring the four most intense Eu centred transitions with 265 nm excitation.

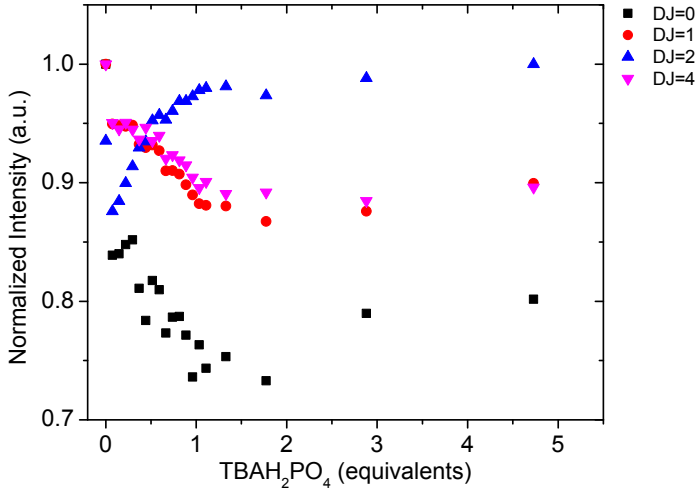

Figure S45. Titration of a 10^{-5}M solution of Eu-rotaxane with $TBAH_2PO_4$ (10^{-3}M) in 1:1 DCM/MeOH followed monitoring the four most intense Eu centred transitions with 265 nm excitation.

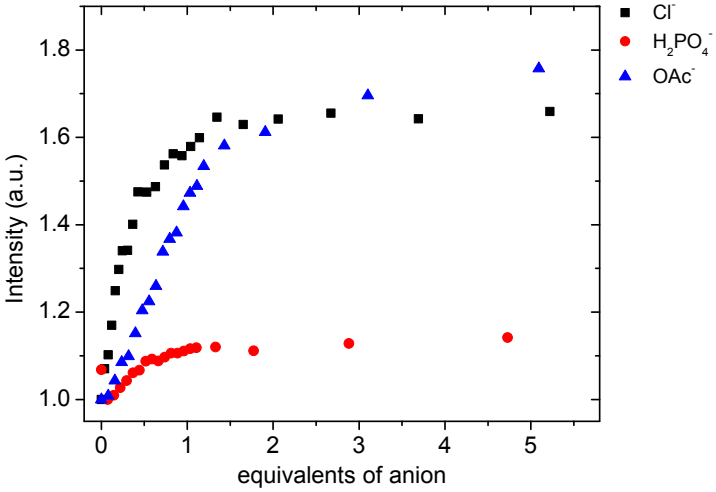

Figure S46. Comparison of a 10^{-5}M solution of Eu-rotaxane ΔJ=2 emission upon addition of chloride, acetate and dihydrogenphosphate (10^{-3}M) in 1:1 DCM/MeOH.

Binding of anions by the Eu rotaxane Eu·1 in 1:1 dichloromethane/methanol – the hypersensitive ΔJ=2 transition

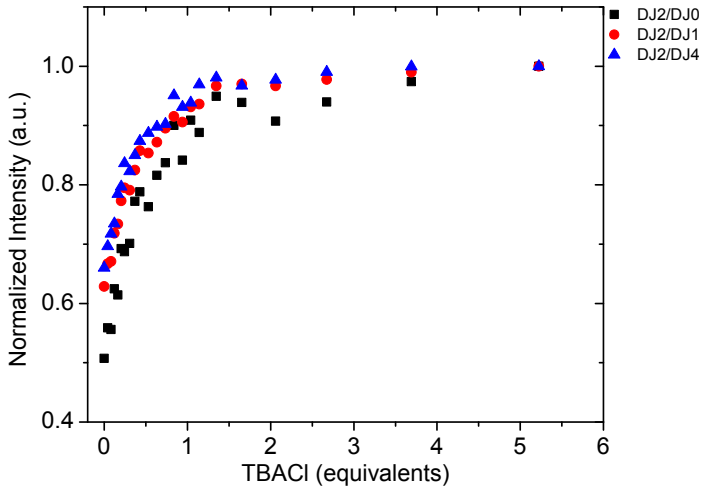

Figure S47. Titration of a 10^{-5}M solution of Eu-rotaxane with TBACl (10^{-3}M) in 1:1 DCM/MeOH followed monitoring the intensity ratio of Eu centred transitions with 265 nm excitation.

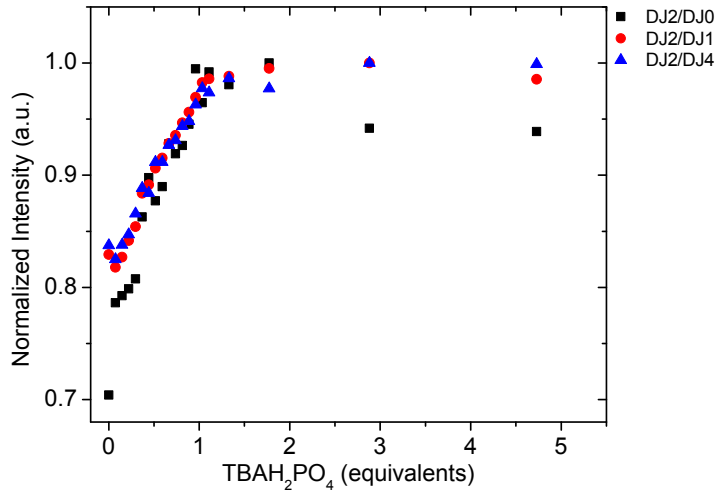

Figure S48. Titration of a 10^{-5}M solution of Eu-rotaxane with $TBAH_2PO_4$ (10^{-3}M) in 1:1 DCM/MeOH followed monitoring the intensity ratio of Eu centred transitions with 265 nm excitation.

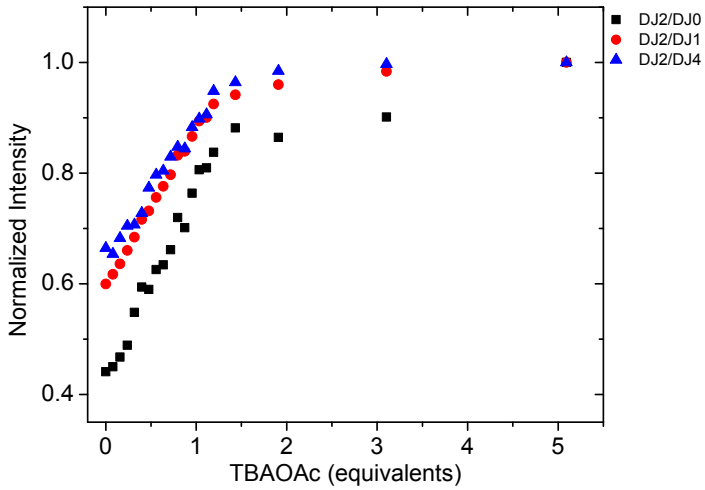

Figure S49. Titration of a 10^{-5}M solution of Eu-rotaxane with TBAOAc (10^{-3}M) in 1:1 DCM/MeOH followed monitoring the intensity ratio of Eu centred transitions with 265 nm excitation.

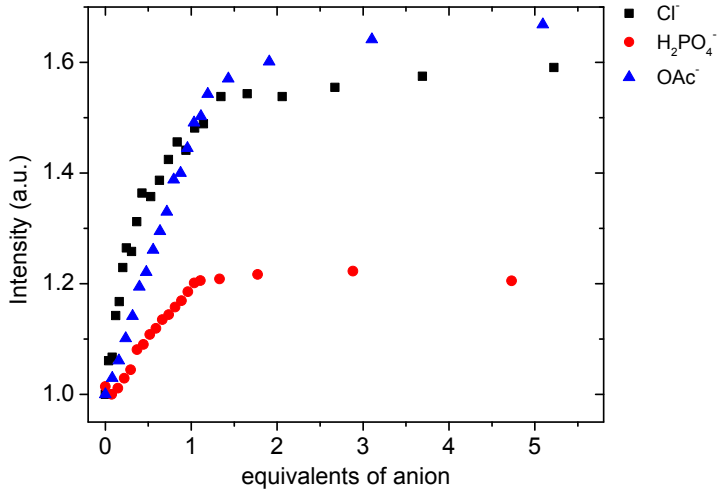

Figure S50. Comparison of the *ΔJ2/ΔJ1* intensity ratios of a 10^{-5}M solution of Eu-rotaxane upon addition of chloride, acetate and dihydrogenphosphate (10^{-3}M) in 1:1 DCM/MeOH.

Binding of anions by the Eu rotaxane Eu.1 in 1:1 dichloromethane/methanol – Dynafit results

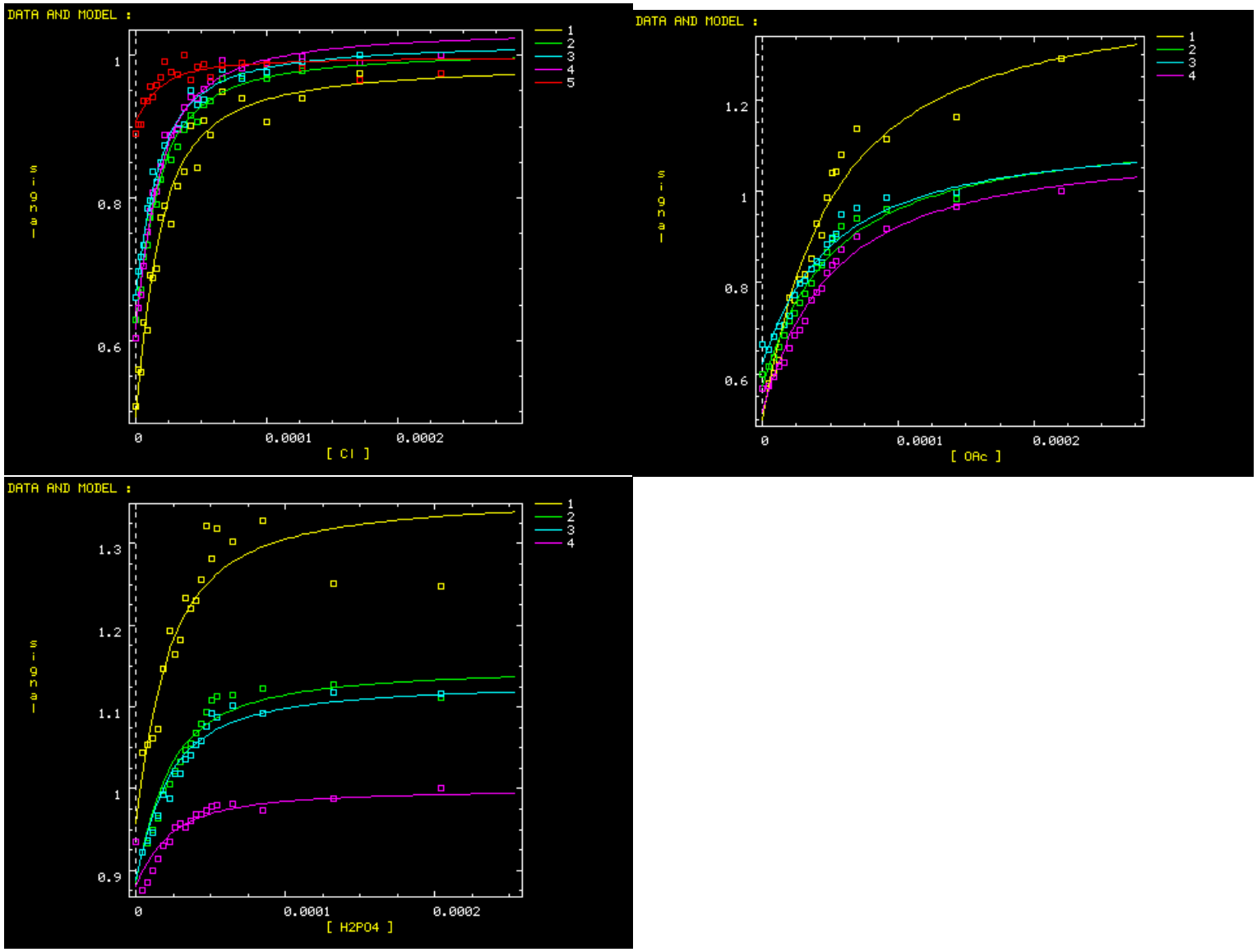

Figure S51. Dynafit output of the titration of Eu-rotaxane with chloride, acetate and dihydrogenphosphate in 1:1 DCM/MeOH. Data (squares) are intensities of the emission signal and/or the intensity ratio (ΔJ=2/ΔJ=N) upon addition of anion for several europium transitions, while fits (lines) are obtained using a 1:1 binding model.

Binding of anions by the model compound 6 in 1:1 dichloromethane/methanol – spectra

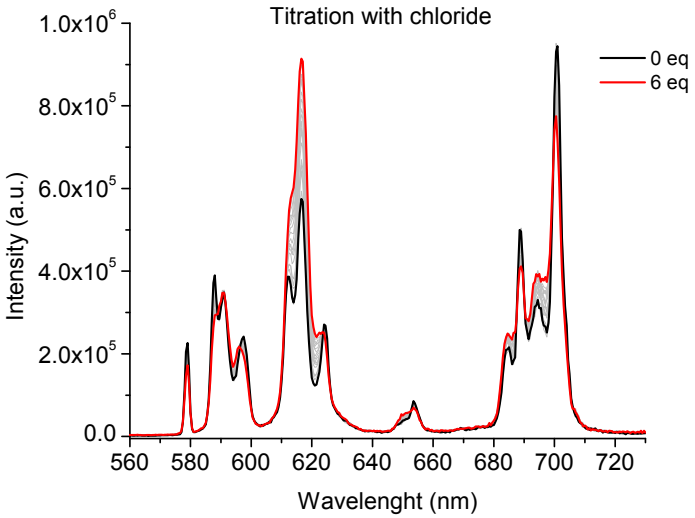

Figure S52. Changes in Eu-centred emission of the model compound **4** (10^{-5}M, 1:1 DCM/MeOH) upon addition of TBACl (0 to 6 equivalents) with 265 nm excitation.

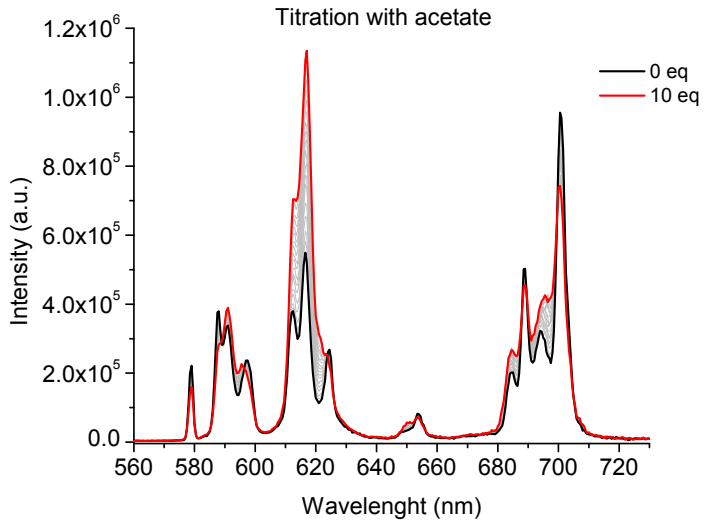

Figure S53. Changes in Eu-centred emission of the model compound **4** (10^{-5}M, 1:1 DCM/MeOH) upon addition of TBAOAc (0 to 10 equivalents) with 265 nm excitation.

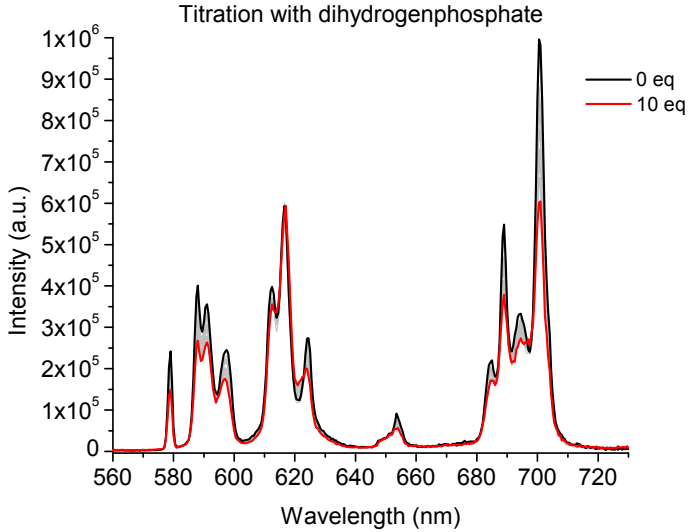

Figure S54. Changes in Eu-centred emission of the model compound **4** (10^{-5}M, 1:1 DCM/MeOH) upon addition of $TBAH_2PO_4$ (0 to 10 equivalents) with 265 nm excitation.

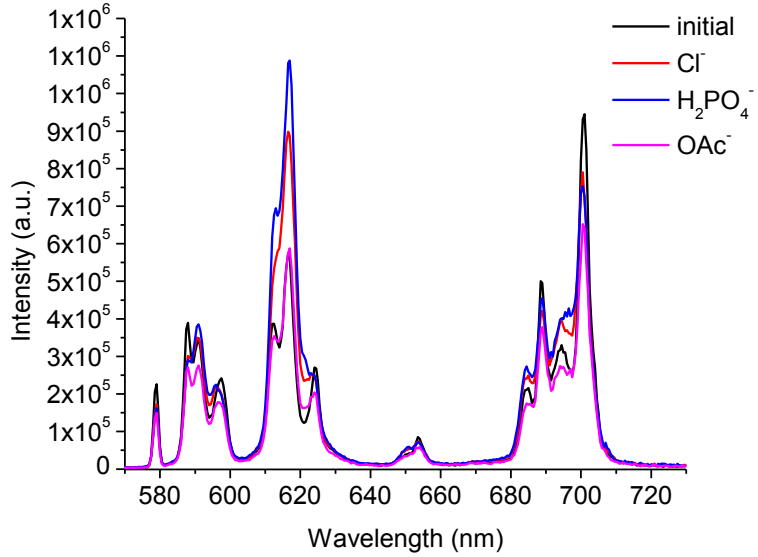

Figure S55. Overlay of the changes in Eu-centred emission of the model compound **4** upon addition of chloride (2 eq.), acetate and hydrogenphosphate (8 eq.) in 1:1 DCM/MeOH.

Binding of anions by the model compound 6 in 1:1 dichloromethane/methanol – intensities

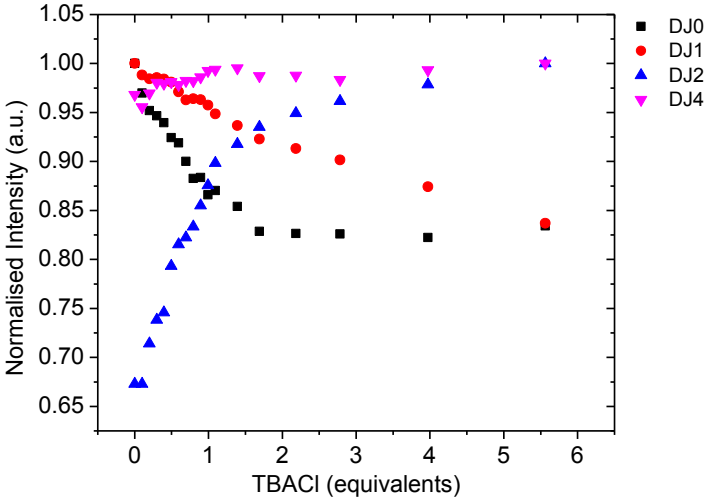

Figure S56. Titration of a 10^{-5}M solution of the model compound **4** with TBACl (10^{-3}M) in 1:1 DCM/MeOH followed monitoring the four most intense Eu centred transitions with 265 nm excitation.

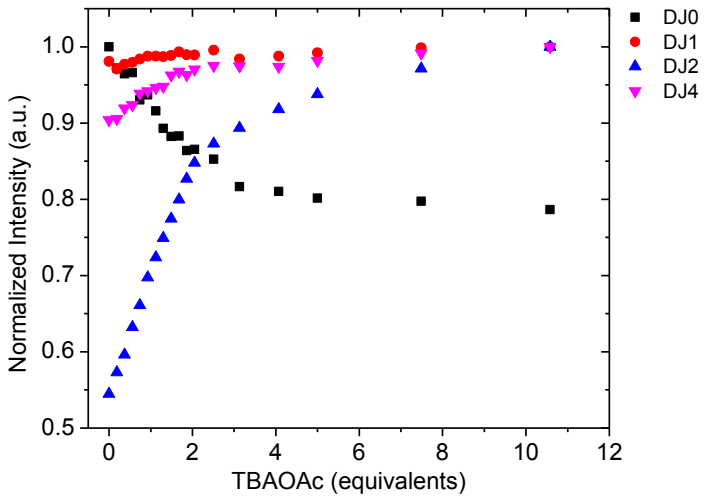

Figure S57. Titration of a 10^{-5}M solution of the model compound **4** with TBAOAc (10^{-3}M) in 1:1 DCM/MeOH followed monitoring the four most intense Eu centred transitions with 265 nm excitation.

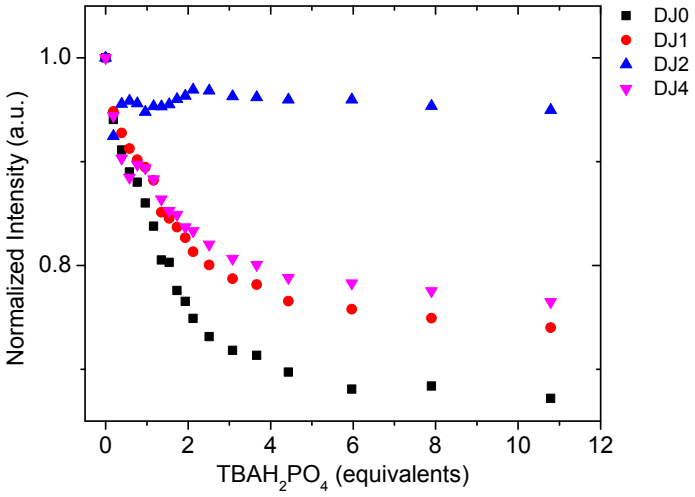

Figure S58. Titration of a 10^{-5}M solution of the model compound **4** with $TBAH_2PO_4$ (10^{-3}M) in 1:1 DCM/MeOH followed monitoring the four most intense Eu centred transitions with 265 nm excitation.

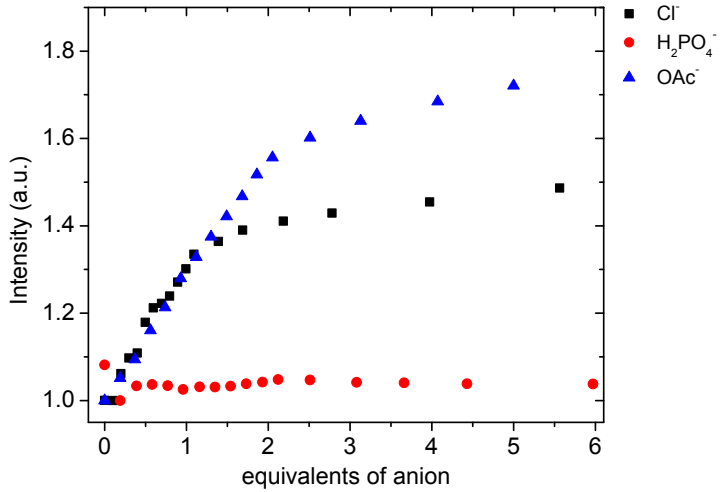

Figure S59. Comparison of a 10^{-5}M solution of the model compound **4** ΔJ=2 emission upon addition of chloride, acetate and dihydrogenphosphate (10^{-3}M) in 1:1 DCM/MeOH.

Binding of anions by the model compound 6 in 1:1 dichloromethane/methanol – the hypersensitive ΔJ=2 transition

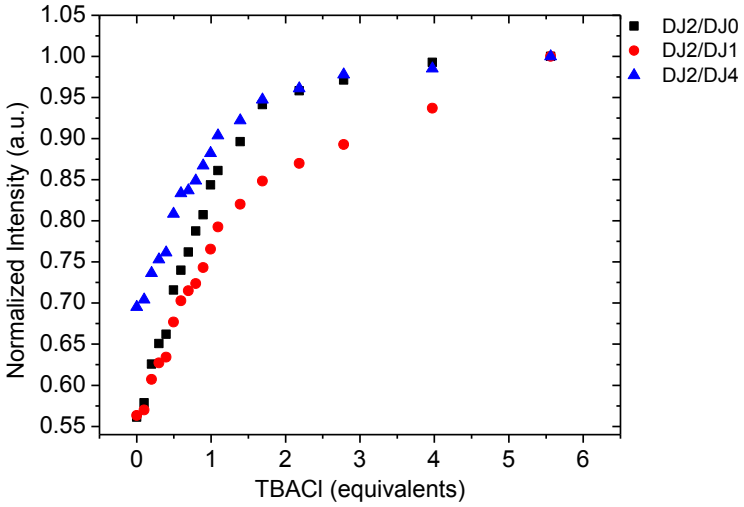

Figure S60. Titration of a 10^{-5}M solution of model compound **4** with TBACl (10^{-3}M) in 1:1 DCM/MeOH followed monitoring the intensity ratio of Eu centred transitions with 265 nm excitation.

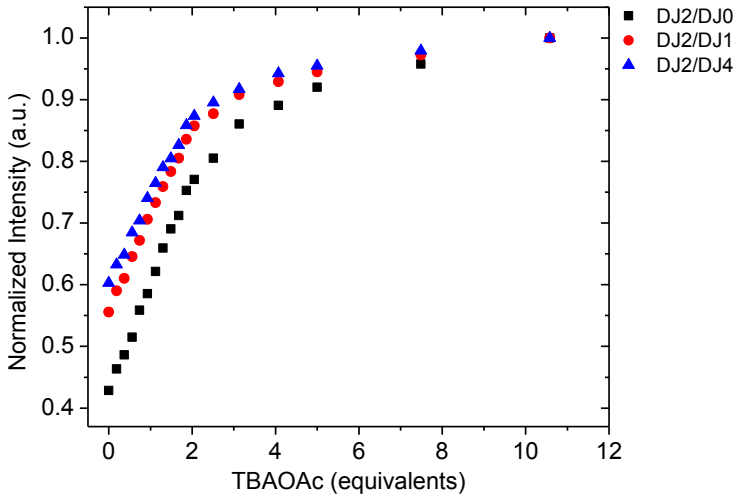

Figure S61. Titration of a 10^{-5}M solution of model compound **4** with TBACl (10^{-3}M) in 1:1 DCM/MeOH followed monitoring the intensity ratio of Eu centred transitions with 265 nm excitation.

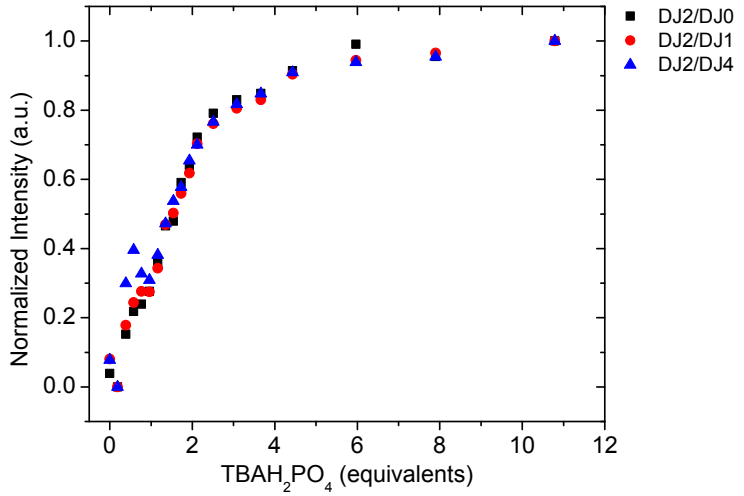

Figure S62. Titration of a 10^{-5}M solution of model compound **4** with $TBAH_2PO_4$ (10^{-3}M) in 1:1 DCM/MeOH followed monitoring the intensity ratio of Eu centred transitions with 265 nm excitation.

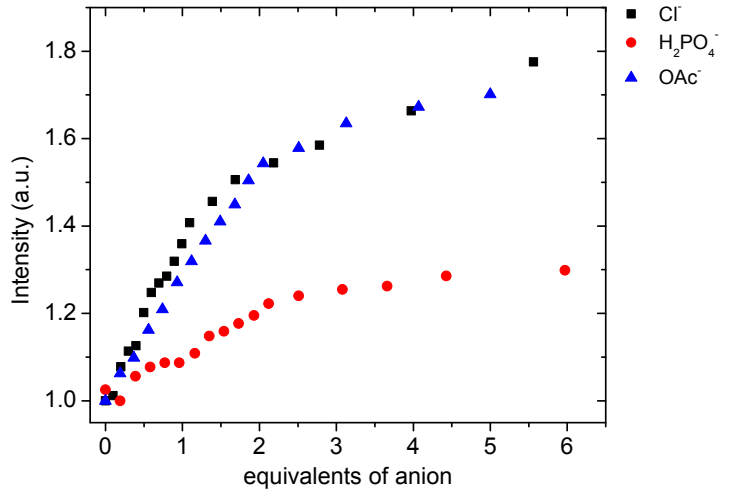

Figure S63. Comparison of the *ΔJ2/ΔJ1* intensity ratios of a 10^{-5}M solution of model compound **4** upon addition of chloride, acetate and dihydrogenphosphate (10^{-3}M) in 1:1 DCM/MeOH.

Binding of anions by the model compound 6 in 1:1 dichloromethane/methanol – Dynafit results

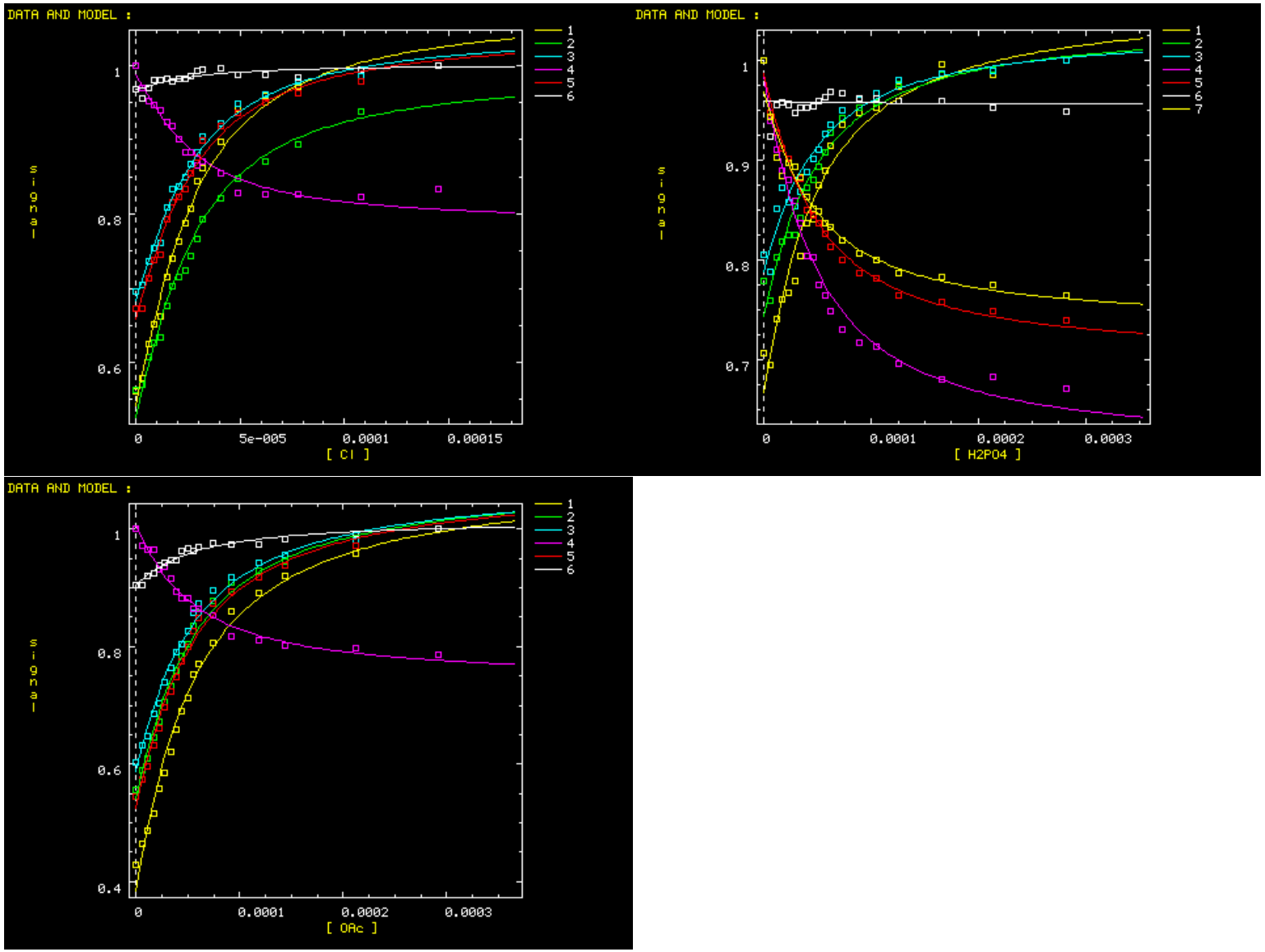

Figure S64. Dynafit output of the titration of the model compound with chloride, acetate and dihydrogenphosphate in 1:1 DCM/MeOH. Data (squares) are intensities of the emission signal and/or the intensity ratio (**ΔJ=2**/ΔJ=N) upon addition of anion for several europium transitions, while fits (lines) are obtained using a 1:1 binding model.

1. J. A. Wisner, P. D. Beer, M. G. B. Drew and M. R. Sambrook, *J. Am. Chem. Soc.*, 2002, 124, 12469-12476.
2. L. M. Hancock and P. D. Beer, *Chem. Eur. J.*, 2009, 15, 42-44.
3. M. Tropiano, N. L. Kilah, M. Morten, H. Rahman, J. J. Davis, P. D. Beer and S. Faulkner, *J. Am. Chem. Soc*, 2011, 133, 11847-11849.
4. Barral, K.; Moorhouse, A. D.; Moses, J. E. *Org. Lett.* 2007, *9*, 1809-1811.
5. M. J. Hynes, *J. Chem. Soc. Dalton Trans.*, 1993, 311-312.
6. J. Cosier, A. M. Glazer, *J. Appl. Crystallogr.* 1986, *19*, 105-107.
7. *CrystalClear: An Integrated Program for the Collection and Processing of Area Detector Data,*; Rigaku Corporation, 1997-2002.
8. A. Altomare, G. Cascarano, C. Giacovazzo, A. Guagliardi, M. C. Burla, G. Polidori, M. Camalli, *J. Appl. Crystallogr.,* 1994, *27*, 435.
9. P. W. Betteridge, J. R. Carruthers, R. I. Cooper, K. Prout, D. J. Watkin, *J. Appl. Crystallogr.,* 2003, *36*, 1487.
10. A. L. Spek, *J. Appl. Crystallogr.* 2003, *36*, 7-13.